Elemental Diffusion Due to Annealing Conditions and its Effect on the Degradation of Perovskite Solar Cell Devices

A Major Qualifying Project
Submitted to the Faculty of
WORCESTER POLYTECHNIC INSTITUTE
In partial fulfillment of the requirements for the
Degree of Bachelor of Science

By

Zoe Mutton

Date:
May 13th 2021

Proposal Submitted to:

Professor Nancy A. Burnham,
Professor Oluwaseun K. Oyewole,
Professor Winston O. Soboyejo
Worcester Polytechnic Institute

Abstract

As climate change worsens, improvements in renewable energy sources become increasingly important. Perovskite solar cells (PSCs) are a promising type of solar cell, but currently have poor lifetimes that exclude them from commercial use. The goal of this project was to develop a method to analyze the diffusion of constituent elements across the layers of PSCs to aid in the understanding of device degradation. Results agree with the literature, indicating that this method is viable for use in future research.

Acknowledgements

I would like to thank my advisors for their continuous encouragement over the course of this project. Thank you to Prof Wole for providing the financial support for the experiments and direction on learning the necessary materials science background. Thank you to Prof Kenny, Juan Martin Hinostroza-Tamayo, and other members of the Energy Group for their assistance in the lab. Thank you to the newest doctor in the group, Deborah Oyewole, for the time she took out of her busy schedule to help me collect SEM data. And finally, thank you Prof Nancy for the continual advice and insight on results, and concern for this report and the entire project.

Table of Contents

1.0 Introduction

While cycles of climate change have been occurring throughout environmental history, it is undeniable that humans have accelerated the temperature increase such that the planet will quickly become uninhabitable. By 2050, the air will be so polluted that it will be dangerous for humans to go outside. The oceans act as a huge carbon sink, but ocean acidification will destroy their ecosystems, accelerating global warming even further. Rising sea-levels will displace countless people, and disease-carrying mosquitoes will be prevalent having flourished in the warmer climate. (Figueres, 2020) The consequences of centuries of inaction are becoming apparent, and if this trend is continued, it will reach a point of no return. Therefore, a solution must be worked towards, and renewable energy is a promising first step.

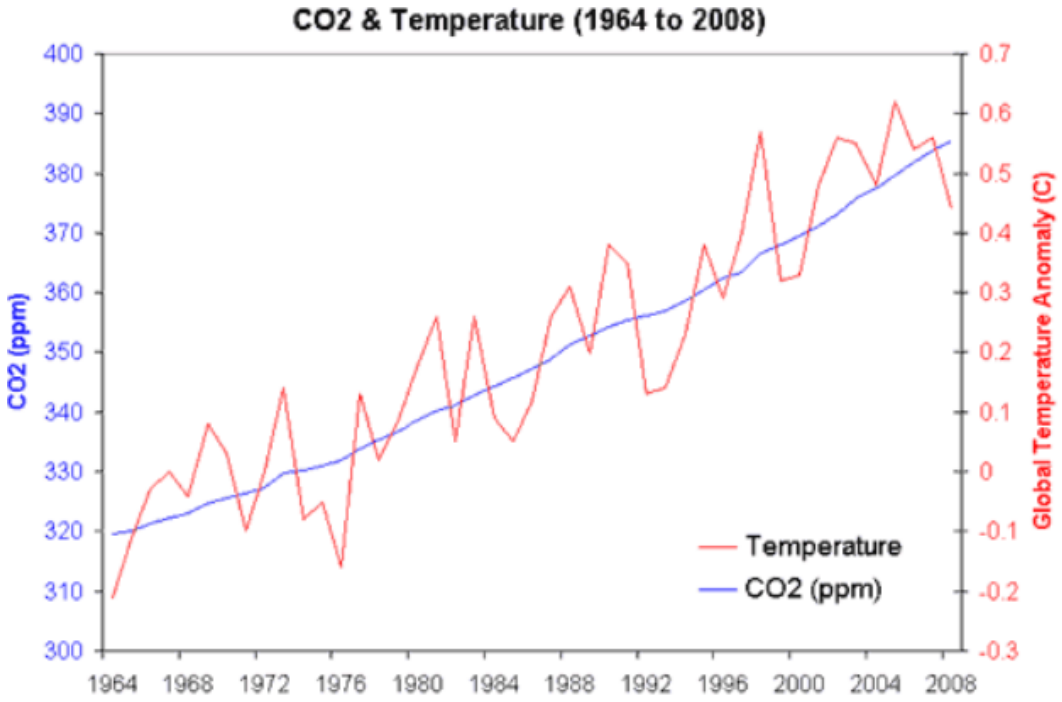

Figure 1: *Atmospheric concentration of CO2 and the global temperature anomaly over time. CO2 concentrations are increasing due to humans, and there is a clear correlation that this is causing the global temperature to rise. ("Undeniable signs," 2020).*

To facilitate the energy transition from fossil fuels to renewables, higher efficiencies and government funding for research and implementation are of utmost importance. However, at the current rate of development, it is not likely that the world will meet the goals of the Paris Agreement. Strategies to accelerate the transition involve improving the existing technologies by either scaling up deployment or overcoming obstacles to commercialization. (Gielen, 2019. "The Paris Agreement," n.d.) Another barrier to the energy transition is the lobbying power of gas and oil companies. To relieve this political pressure, renewables must become overwhelmingly impressive in efficiency and cost. (Gabbatiss, 2019)

From its first deployment in 1954, solar energy has been one of the leading prospects for generating renewable energy. Though it took great effort and thorough development -jumping from 4% to 14% to 20% efficiency from its beginnings to 1985- investment in solar energy has been increasing as the consequences of fossil fuels are becoming more apparent. As research has improved, silicon solar cells (SSCs) have even reached 25% efficiency. (Richardson, 2018) With all these improvements, however, there are still unfortunately some drawbacks. SSCs are brittle, thick, and heavy. They require extremely high temperatures to convert silicon dioxide into pure silicon, making them expensive, and most importantly, SSCs have plateaued at 25% efficiency for 15 years, as shown in Figure 2 (indicated by the pink circle). (Carbeck, 2016)

One promising alternative which solves these problems is perovskite solar cells (PSCs). PSCs are fabricated at lower temperature, and the resultant films are much thinner and lighter than SSCs. They have also gone from 4% to 26% efficiency in just 20 years (circled in red in Figure 2). This is due to the material possessing both a good absorption spectrum and good charge carrier lifetime and mobility. As exciting as they may be, PSCs still have many obstacles that prevent them from being used commercially, the sum of which resulting in poor device lifetimes of 6 to 12 months, with significantly diminished efficiencies.

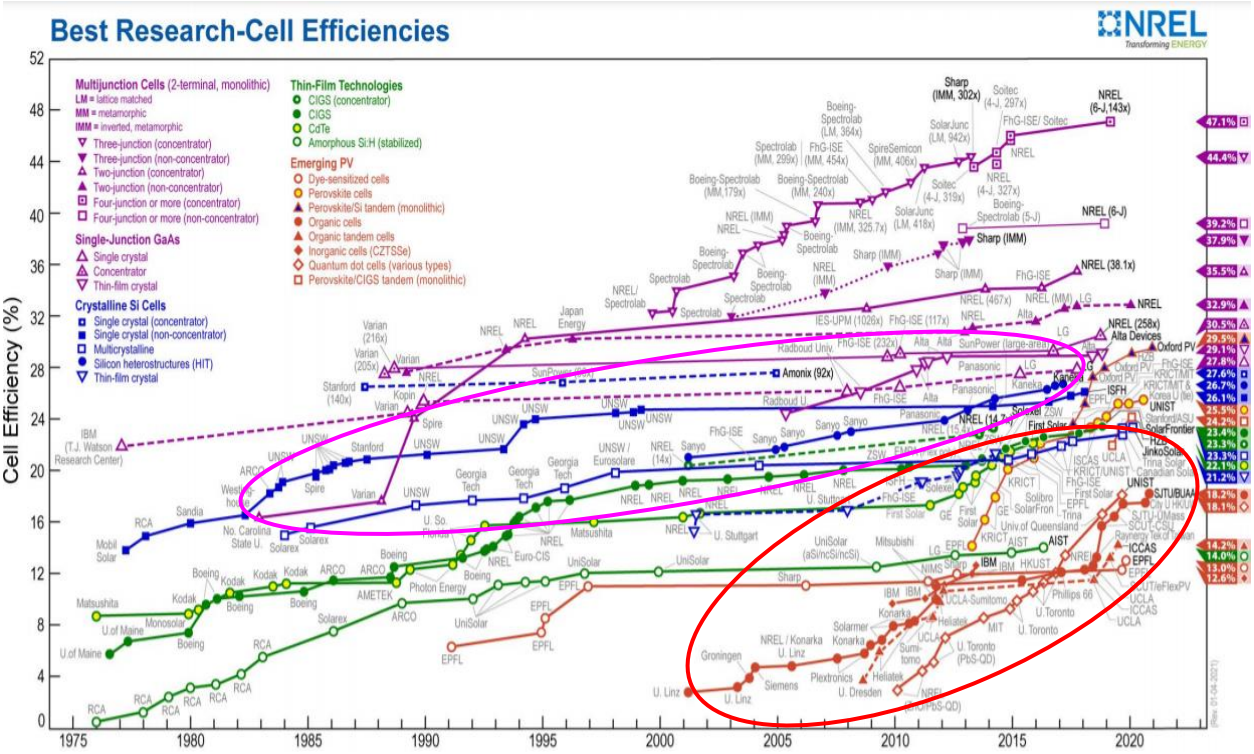

Figure 2: *Efficiency over time for different types of solar cells. SSCs (blue) have plateaued since 2000, while PSCs (orange) have shown significant growth in just 20 years. (NREL, 2021)*

This report begins with a background on diffusion and the physics of PSCs, and a review of the current problems and research that has been done on PSC stability. Next is the methodology, which describes device fabrication and the specifics of this project in more detail, as well as the data analysis method which was a key part of the work that was done. From there, the results and limitations are discussed, followed by the conclusion and opportunities for future work.

2.0 Literature Review

2.1 Introduction to Diffusion and its Role in Solar Cell Physics

Diffusion is traditionally thought of as a substance passively moving through a liquid or gas medium from high to low concentration to create a uniform distribution, such as a spray of perfume slowly filling a room. However, diffusion can still take place in solids despite their rigidity; defects and vacancies in the crystal lattice allow for atoms to jump from one site to the next within a material. Diffusion of charges can also take place, such as when an electron is excited and exits the valence band, and the hole it leaves behind can propagate throughout the lattice. These are both important in solar cell physics, as driving the separation of these excitons is fundamental to their function, and the diffusion of each layer's constituent atoms can lead to serious degradation of these devices.

2.1.1 Diffusion in Solids

In solids, diffusion occurs when atoms move to adjacent vacancies or from one interstitial site to another. The diffusion of atoms within the crystal lattice of solids can lead to macroscopic results, as shown in Figure 3; two metal solids are welded together (A), then after a long period of time, the diffusion of the atoms shifts the position of the initial weld (B). (Abbaschian, 2009)

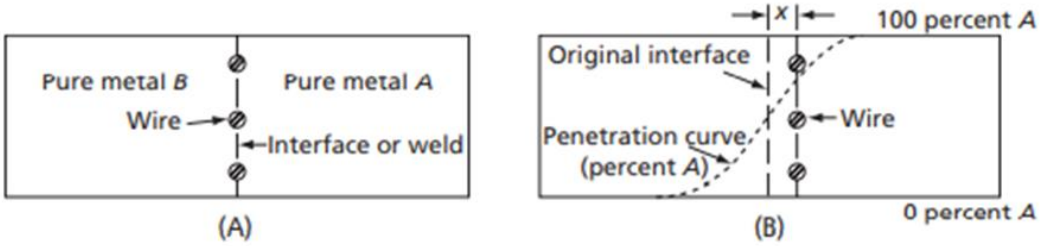

Figure 3: *(A) The initial state of two metal bars welded together. (B) The final state of the bar after diffusion has occurred. The original interface has been shifted by the movement of atoms. (Abbaschian, 2009)*

The rate at which two elements diffuse into each other is dictated by Fick's first law, $J = -D\frac{\Delta c}{\Delta x}$, where J is the flux, D is the diffusivity constant, and $\Delta c/\Delta x$is the concentration gradient. (Askeland, 1996) The diffusivity constant is defined by the Arrhenius equation, proposed by Svante Arrhenius in 1889: $D = D_0 e^{-Q/RT}$, where D_0 is the maximal diffusivity constant (at an

infinite temperature), R is the universal gas constant, T is the temperature, and Q is the activation energy required for atoms to make a jump. ("Mass Diffusivity," 2021) Since activation energy depends on the strength of atomic bonding, it is lower for materials with low melting points. Atoms also have an easier time diffusing through open crystal structures, such as grain boundaries and free surfaces. Grain boundaries tend to have a larger effect on diffusion, because they form a network throughout the sample, and there is generally more grain boundary surface area than free surface area. (Askeland, 1996)

The diffusivity constant can be determined through experimentation; simply measure the distance the original interface, x, has moved over a given amount of time, t. From this, the marker velocity can be determined by $v = \frac{x}{2t}$. Then D can be calculated using the concentration gradients of each material. (Abbaschian, 2009)

By taking the common logarithm ($2.3log_{10}(x) = ln(x)$) of each side of the Arrhenius equation,

$$logD = -\frac{Q}{2.3RT} + logD_0,$$

a semi-log plot can be obtained to show the temperature dependence of the diffusivity constant, shown in Figure 4, where it shows a greater diffusivity constant for higher temperatures. The dependent variable is D, the y-intercept is $logD_0$, the independent variable is 1/T, and the slope is -Q/2.3R. Using experimental data, this can be used to find D_0 and the activation energy for ion migration. (Abbaschian, 2009)

Temperature *K*	Self-Diffusion Coefficient *D*	$\frac{1}{T}$	log *D*
700	1.9×10^{-15}	1.43×10^{-3}	−14.72
800	5.0×10^{-14}	1.25×10^{-3}	−13.30
900	6.58×10^{-13}	1.11×10^{-3}	−12.12
1000	5.00×10^{-12}	1.00×10^{-3}	−11.30
1100	2.68×10^{-11}	0.91×10^{-3}	−10.57

Table 1: Experimental diffusivity data used in Figure 4. (Abbaschian, 2009)

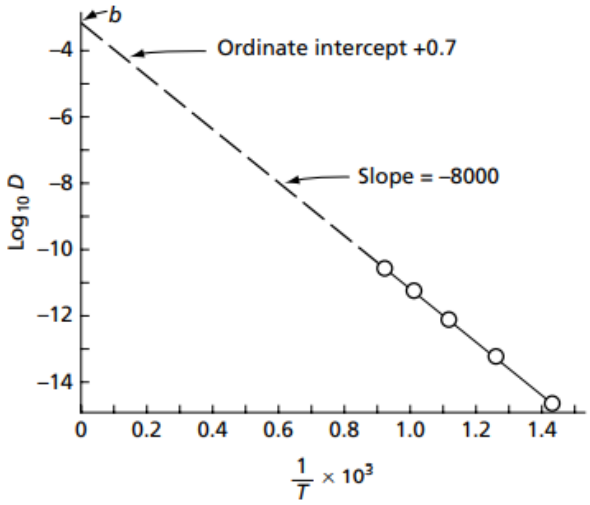

Figure 4: *An example of a semi-log plot to show the temperature dependence of the diffusivity constant. The experimental data is shown in Table 1. For this data,* $D_0 = e^{0.7}$*, and the activation energy can be found by solving* $-8000 = -2.3Q/R$. (Abbaschian, 2009)

Diffusion length, a quantitative representation of "amount" of diffusion, can be calculated by $l = 2\sqrt{Dt}$. ("Diffusion," 2021)This indicates that more diffusion will occur at longer timescales and higher temperatures.

2.1.2 Charge Diffusion in Solar Cells

In order for a solar cell to harvest light and convert it to electricity, it must 1) absorb a photon and generate an exciton, 2) separate the electrons and holes, and 3) extract the electrons to an external circuit. ("Solar Cell," 2021) This section will discuss aspects of the second and third steps.

In traditional SSCs, the silicon is doped to have a positive (p) and a negative (n) side. This is called the p-n junction, and generates an electric field to drive charge separation; the negative electrons are attracted to the p-side, and the positive holes move to the n-side, as shown in Figure 5. (Würfel, 2005)

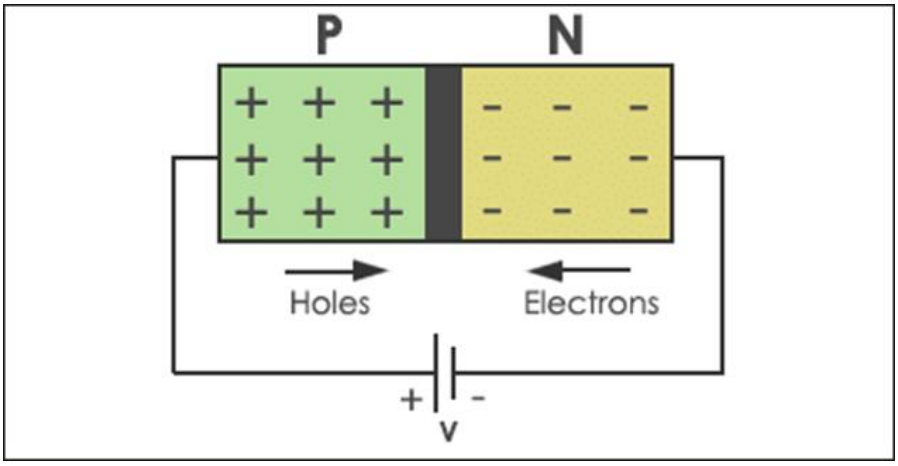

Figure 5: *A p-n junction. The holes move towards the n-side, and the electrons move towards the p-side. (Nasir, 2021)*

Recombination is when an electron and hole recombines to emit a photon, and must be minimized within solar cells to maximize efficiency. Some recombination occurs as the charge carriers diffuse past each other in the p-n junction, forming a neutral depletion zone. (P-n junction," 2021)

Another component that contributes to solar cell efficiency is the charge carrier mobility, μ, which is how well a charge can move through a material. This is mostly determined by the material's purity. A charge's drift velocity in the presence of an electric field, E, is $v_D = \mu E$. (Spies, 2017) The faster a charge can move through a material and be extracted to an external circuit, there is less time and a lower probability for recombination to occur.

2.2 Perovskite Solar Cell Physics

In recent years, PSCs have attracted attention in the scientific community because of their high absorption and high efficiency, and because perovskite materials are much easier and cheaper to manufacture than traditional SSCs. [reference] One of the main reasons that PSCs are not used commercially is that they are unstable, with device lifetimes of six months to a year, making it important to identify and prevent the factors that accelerate their degradation.

2.2.1 Device Structure and Layer Functions

A PSC device consists of a thin film perovskite layer sandwiched between an electron transport layer (ETL) and a hole transport layer (HTL), with metal electrodes to connect it to an external

circuit. The specific PSC architecture used for this project is shown in Figure 6. Fluorine-doped tin oxide (FTO) coated glass is used as the substrate, with the FTO and gold functioning as electrodes.

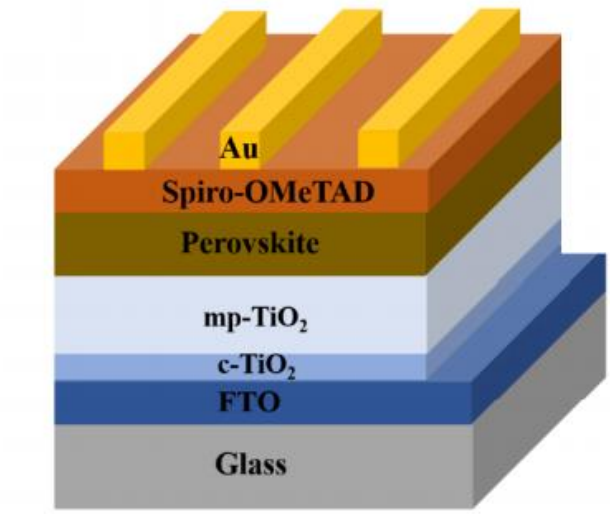

Figure 6: *The architecture of a PSC device. FTO and Au are the metal electrodes, the TiO_2 layers form the ETL, and the spiro layer is the HTL.*

The compact TiO_2 (c-TiO_2) and the mesoporous TiO_2 (mp-TiO_2) function as the ETL, where the mp-layer can help influence the formation of perovskite crystals, and improves contact with the perovskite layer when the device is subjected to mechanical pressure. (Oyelade, 2020) The perovskite layer is the light-harvesting layer, and the sprio-OMeTAD (spiro) functions as the HTL. (Lopez-Varo, 2018)

2.2.2 Charge Carrier Generation, Transport, and Recombination

Like all solar cells, PSCs convert sunlight into electricity through the photovoltaic effect; the perovskite acts as the light-harvesting layer, and the ETL and HTL aid in charge carrier separation. In SSCs, the p-n junction is what allows for the separation of electron-hole pairs, as discussed in sections 2.1.2. Charge separation is similar in PSCs, however the electric field is created by the vastly different work functions of the HTL and ETL. (Lopez-Varo, 2018) Once the electrons and holes are separated, the electrons must diffuse from the perovskite layer, through the ETL, and then travel through an external circuit to power a load before recombining with the holes in the HTL.

In a solar cell device, the two main factors of efficiency are how well the material can absorb photons, and how well the device can transport the excited electrons to an external circuit (essentially preventing premature recombination). This is dictated firstly by band gap and absorption spectrum, and secondly by charge carrier lifetime, mobility, and diffusion length, all of which PSCs excel at. (Kirchartz, 2018) However, having both strong absorption and long carrier lifetimes makes perovskite a perplexing material, as these properties are typically mutually exclusive, being dependent on the type of band gap a material has.

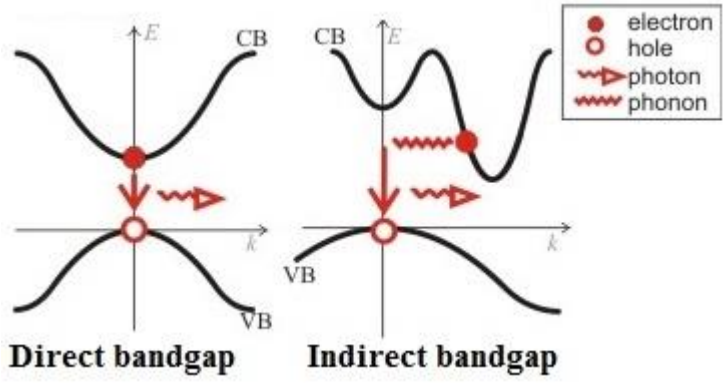

Figure 7: *The difference between direct and indirect band gaps. The conduction and valence bands have the same k-vectors for a direct band gap, and different k-vectors for an indirect band gap. (Chen, n.d.)*

Band gap type is determined by the relationship between the conduction band and the valence band; each band is characterized by a k-vector, having to do with the momentum of electrons within the crystal lattice. If the k-vectors are the same, there is a direct band gap, and if they are different, it is indirect, as shown in Figure 7. When the k-vectors are different, in order for an electron to transition between the bands, it must go through a transitional state in order to conserve crystal momentum. This involves phonons which can inhibit light absorption, and make the process longer, making the probability of premature recombination lower. This is why direct band gap materials are better at absorbing and emitting light, and those with indirect band gaps have much longer carrier lifetimes. (“Direct and indirect,” 2021)

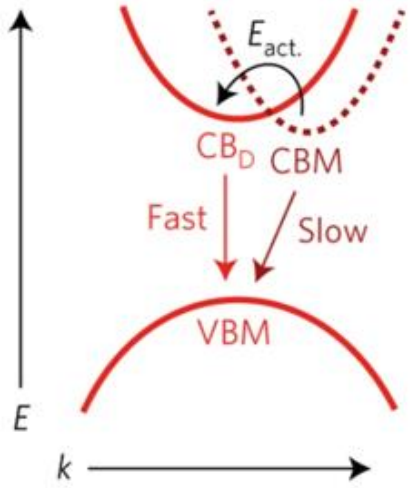

Figure 8: *Rashba splitting of perovskite's band gap. It makes a direct transition on the way up, and an indirect one on the way down. (Hutter, 2017)*

In theoretical calculations, perovskite should have an indirect band gap, but experimentally behaves as if it were a direct band gap material. This is due to Rashba splitting of the conduction band, caused by a local electric field across the Pb atoms, allowing for both direct and indirect transitions to take place, shown in Figure 8. (Wang, 2016) Essentially, when photons are absorbed, electrons are excited through the direct transition, but must recombine through a phonon-assisted pathway. (Hutter, 2017)

2.3 PSC Degradation Factors

There are several factors that contribute to PSC degradation: perovskite's intrinsic instability, under light illumination, and due to oxygen and water vapor. The exact mechanisms of degradation are not well understood, but this section will give an overview of them.

2.3.1 Intrinsic Instability

Each of the other factors discussed work to accelerate the spontaneous decay and evaporation-like process of the perovskite layer. There are two reactions that are viable, shown below, the first being the most likely as it is favored by the kinetics. (Bisquert, 2019)

$$MAPbI_3\,(s) \rightarrow NH_2CH_3\,(g) + HI\,(g) + PbI_2\,(s) \quad (1)$$

$$MAPbI_3\,(s) \rightarrow NH_3\,(g) + CH_3I\,(g) + PbI_2\,(s) \quad (2)$$

Another issue is that I and Pb easily diffuse through the material, with very low vacancy and interstitial migration activation energies of ~0.1 eV and ~0.8 eV, respectively. (Apiroz, 2015) This is due to their relatively low melting points (114C for I, 327C for Pb, compared to 1,414C for Si).

2.3.2 Other Factors

A bit ironically, PSCs will degrade under light, as shown in Figure 9. One study found that under white-light illumination, the valence features are shifted to a lower binding energy due to the surface photovoltage, but after illumination this is only partially reversible, resulting in a high concentration of reduced Pb, and the formation of PbI_2 defects (footnote about PbI_3 being main thing in perovskite). This indicates quenching of the surface, where recombination happens almost immediately after exciton generation. (Zu, 2017)

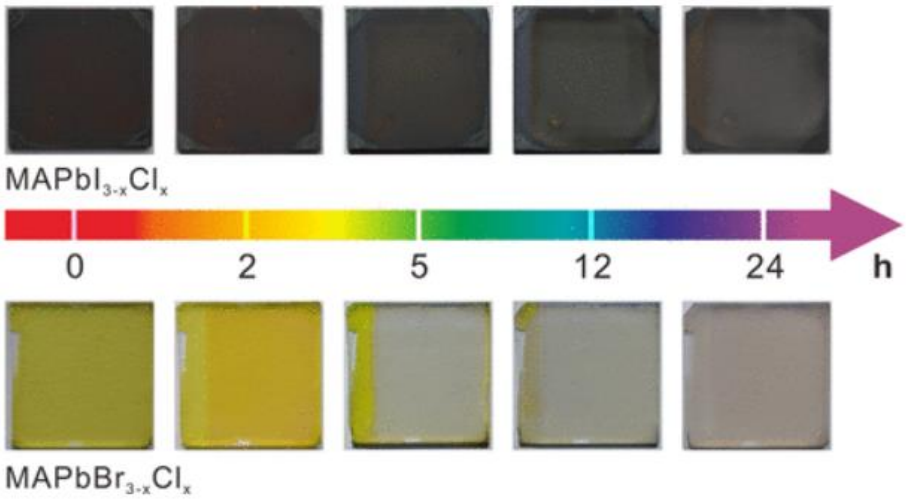

Figure 9: *Optical images of two different PSCs after light illumination. There is a clear change in color, indicating chemical decomposition. (Xu, 2018)*

Oxygen contributes in a similar way, by absorbing the excited electrons to form superoxide (O_2^{-1}) which is highly reactive and reacts with the organic component of the perovskite, accelerating the degradation process.(Ralaiarisoa, 2018) Lastly, water vapor reacts with the inorganic component of the perovskite forming hydrate phases of PbI_2 or simply expediting its production. (Deretiz, 2018)

2.3.3 Some Solutions

Since these factors are so prevalent in the degradation of PSCs, much work has been invested into preventing them. Several studies have found that placing the samples, and even encapsulating them in an N_2 atmosphere, greatly increases device stability. This is thought to be caused by passivation at the surface, preventing gas desorption as shown in the decay reactions. (Mannino, 2017. Deretzis, 2018). Another interesting solution was the implementation of a graphene barrier between the perovskite and the ETL. This was successful at blocking I and Pb migration, as shown in Figure 10. (Bi, 2017)

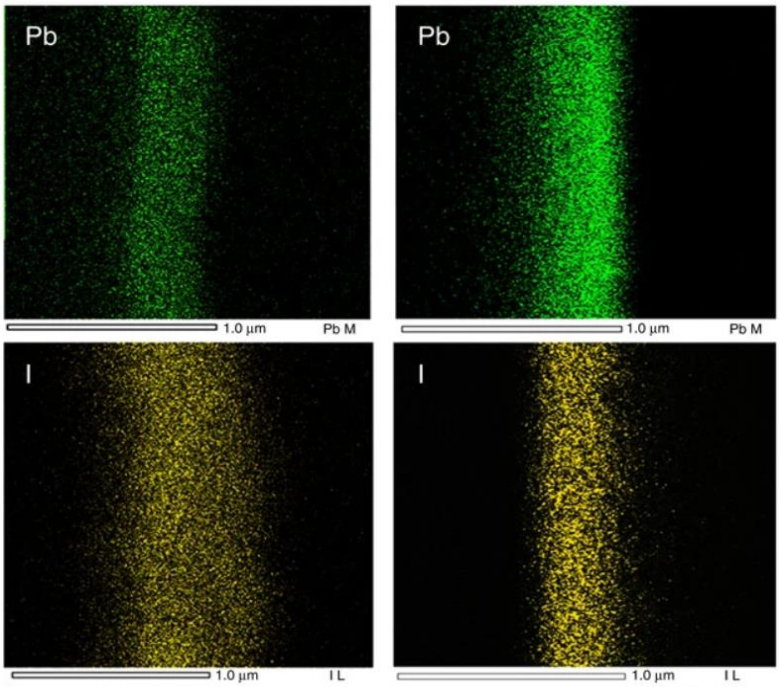

Figure 10: *Energy dispersive spectroscopy (EDS) elemental maps for I and Pb. On the left, without the graphene barrier, on the right, with the graphene barrier. The devices with the graphene barrier show a clear prevention of ion migration. (Bi, 2017)*

The latest development in PSCs stability is a self-assembling monolayer (SAM) to improve the interfacial toughness between the perovskite layer and ETL. Along with preventing morphological degradation, it improved device efficiency from 20.2% to 21.4%, and improved device lifetime. The authors noted that after improving this layer's weakness, attention must be shifted to use SAMs for the next weakest layer. (Dai, 2021)

All of these degradation factors depend on and result in diffusion of the constituent elements of the device. These elements diffuse to layers where they should not be present, and are indicative of morphological damage to the device. The goal of this project is to analyze this diffusion, and determine if there is any relationship with varying annealing conditions.

3.0 Methodology

This section discusses the materials and fabrication methods used to construct each layer of a PSC device, followed by the experimental procedure and data analysis methods used in this project.

3.1 Materials

Each layer of a PSC device requires specific chemicals and tools as a part of its deposition. These are outlined in detail in Appendix 1.

3.2 Fabrication of PSC Devices

The devices used in this project have the same structure that the Energy Group has developed but excludes the HTL and gold cathode as shown in Figure 11. This was done because these layers are expensive and characterization of the perovskite layer was the focus of this project. This part of the experiment required a hot plate, a spin coater, vacuum pump, and compressed nitrogen gas.

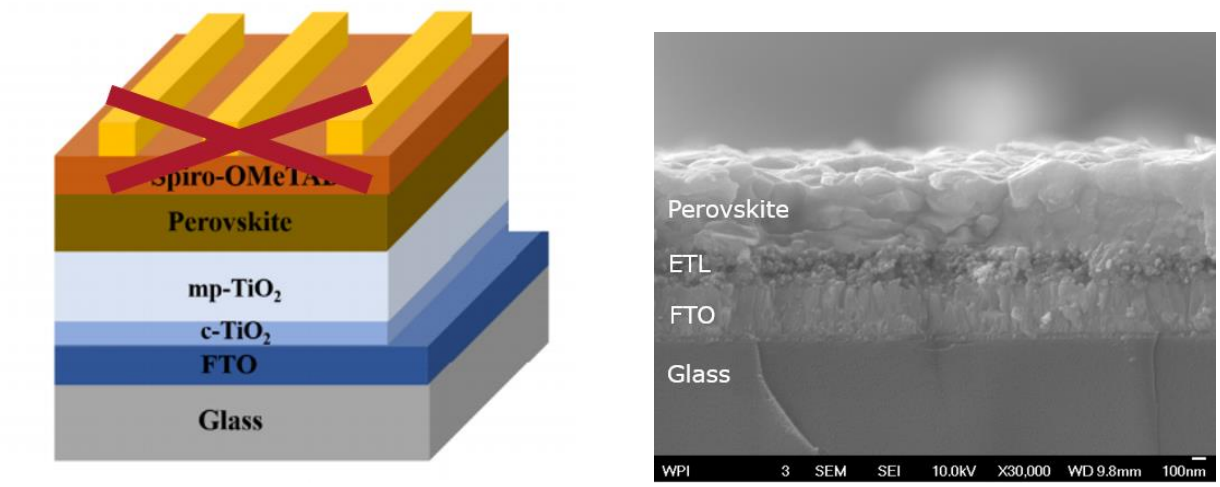

Figure 11: *Device structure for this experiment. On the left, a graphic of device structure with the top two layers excluded. On the right, an SEM image of a physical device. The c- and mp-TiO_2 layers are difficult to distinguish, so they are labeled together as the ETL.*

3.2.1 Cutting and Cleaning Glass Substrate

FTO-coated glass was cut FTO-side-down with a diamond cutter into 12.5 x 22.5 mm rectangles. These were then sonicated in detergent, acetone, and isopropyl alcohol for 15 minutes each before being dried with pressurized air. Finally, the glass slides were placed FTO-side-up in an ozone system cleaner for 10 minutes.

3.2.2 Deposition of Electron Transport Layer

The c-TiO_2 is made by spin-coating and annealing 0.15 M and 0.30 M solutions of titanium diisopropoxide bis(acetylacetonate) dissolved in 1-butanol. First, the 0.15 M solution was spin-coated at 2000 rpm for 30 seconds then annealed at 150C for 5 minutes. Then, the 0.30 M solution was spin-coated with the same parameters and annealed at 500C for 30 minutes.

The mp-TiO_2 is made with a mixture of titania paste and ethanol in a 1:5 weight/weight ratio. This mixture was spin-coated at 4000 rpm for 30 seconds, then annealed in an oven at 500C for 1 hour.

3.2.3 Deposition of Perovskite Layer

There is a two-step deposition process of the perovskite layer. The first layer is a 1.3 M solution of PbI_2 mixed in a DMF:DMSO = 9.5:0.5 in a volume/volume ratio. This was mixed for 2 hours with magnetic stirring at 60C, then filtered before it was spin-coated at 1500 rpm for 30 seconds. After spin-coating, it was annealed at 70C for 1 minute. The second layer is a mixture of FAI, MABr, and MACl (10 mM: 1 mM: 1 mM) dissolved in isopropyl alcohol. This was spin-coated at 1300 rpm for 30 seconds. For fabrication of full devices, this layer is annealed at 130C for 20 minutes, but for this project the annealing conditions were changed as outlined in the next section.

3.3 Experimental Conditions

The goal of this project was to investigate if changing the annealing conditions of the perovskite layer had any effect on elemental diffusion within a PSC device. Two different trials were carried out, one changing the length of annealing time, and the other changing the temperature. For the time trial, 0, 10, 20, and 30 minutes were used, and for the temperature trial, 100C, 120C, 130C, and 140C were used and compared to the 0 minute sample as the control.

3.4 Characterization of Diffusion

A bulk of this project was spent developing a method to characterize the elemental diffusion that was taking place during the annealing process. Before this project, the Energy Group would take energy dispersive spectroscopy (EDS) within each layer to get a weight percent composition as shown in Figure 12.

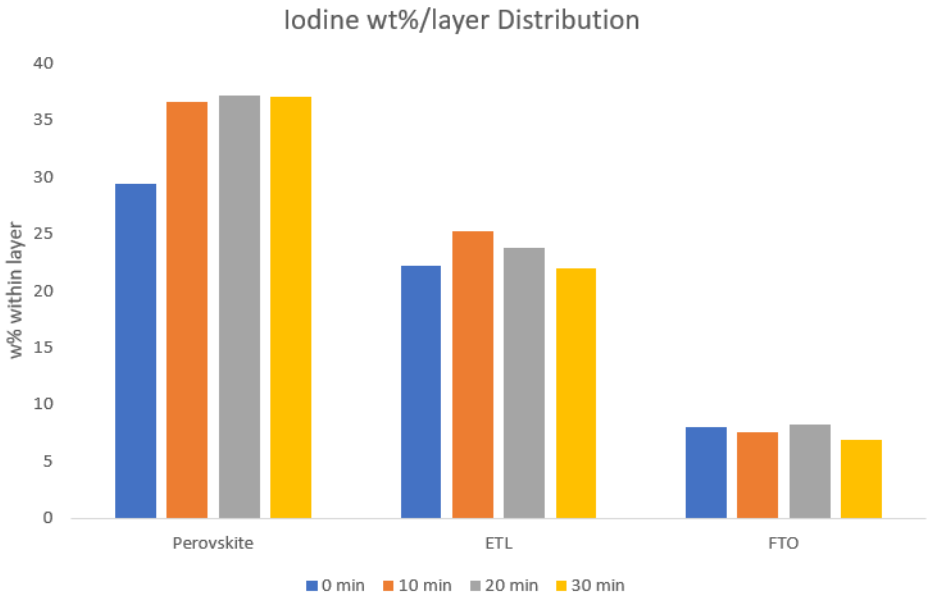

Figure 12: *The weight percent of iodine in each layer for different annealing times. There is no clear trend between different times, and there is no information about layer interfaces.*

While this method was sufficient for other projects in the group, this did not yield enough information for this project; it produced a discrete graph for information within each layer, but did not show what was happening across the whole device or at layer interfaces. The solution to this problem was to use the EDS elemental maps, as discussed in the next section.

3.4.1 Data Analysis of EDS Maps

Along with weight percent composition, EDS can also produce elemental maps to give a spatial distribution of each element, as shown in Figure13. This provides the information that the first method was lacking; continuous information about elemental concentration across the device. However, these images are not easily compared by eye.

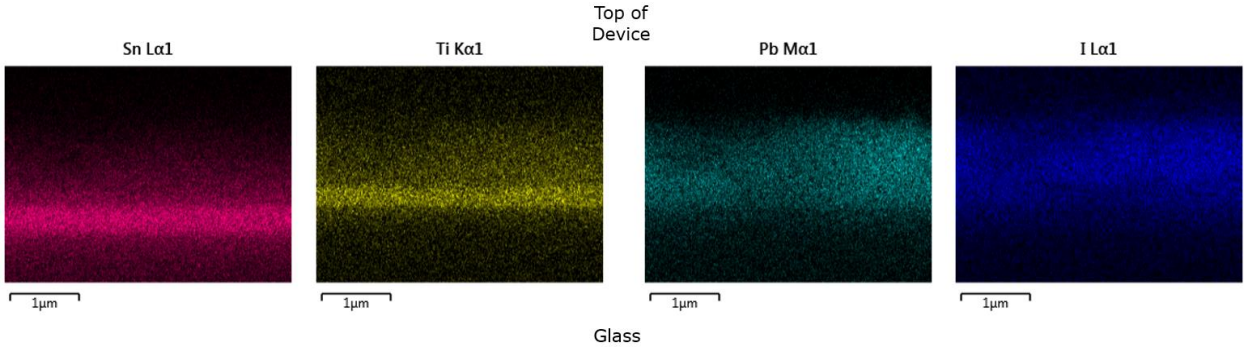

Figure 13: *EDS elemental maps of (left to right), Sn, Ti, Pb, and I. The Sn and Ti show clear bands where the FTO and ETL are, respectively, but still diffuse to other parts of the device. The Pb and I have a much larger spread.*

To better compare this data, these maps were converted to concentration profiles. A Python script was written to obtain the brightness of each pixel, which were then normalized to white (greyscale value of 255). Next, these brightness values were averaged for each column as demonstrated in Figure 14.

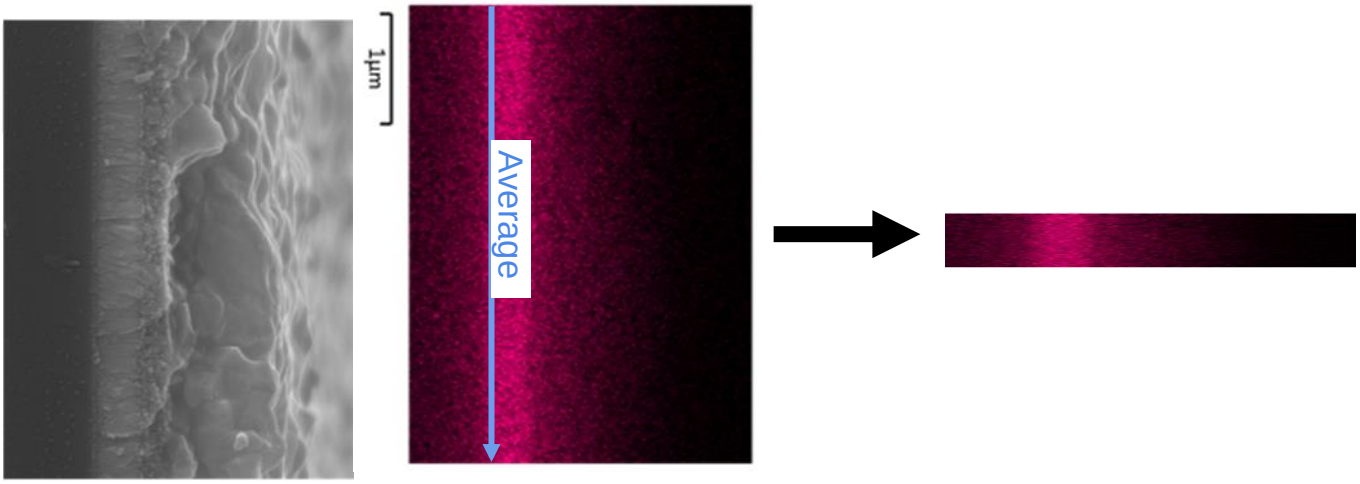

Figure 14: *A visualization of how the images were processed. The average brightness for each column was taken to convert the images into concentration profiles as shown in Figure 15.*

The resultant concentration profile is shown in Figure 15. The horizontal axis is the distance from the bottom of the device (the glass slide) in nanometers, and since these brightnesses were all normalized to white, the vertical axis can be interpreted as a normalized concentration[1].

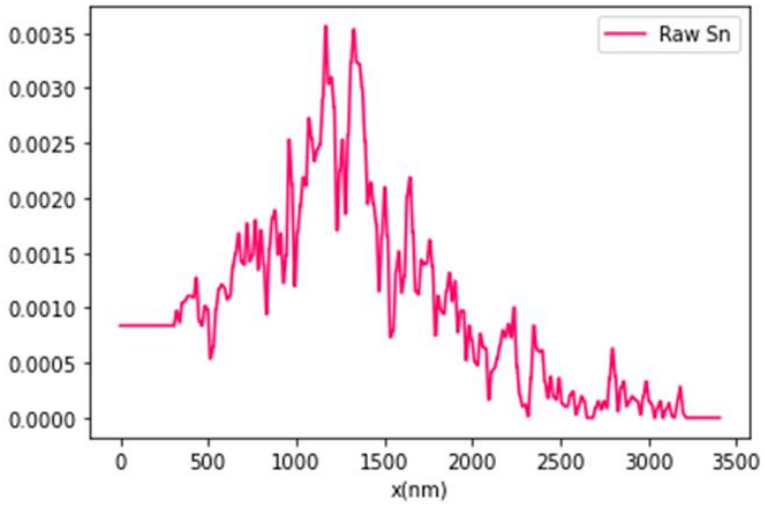

Figure 15: *The raw concentration profile of Sn. The horizontal axis is the distance from the bottom of the device, and the vertical axis can be interpreted as a normalized concentration.*

Another obstacle to this method was that the layers in the EDS maps were vertically offset from each other, as shown in Figure 16. In order to ensure that the concentration profiles were aligned across samples, the distances from the bottom of the image to the glass-FTO interface were measured and used to adjust the concentration profiles as shown in Figure 17.

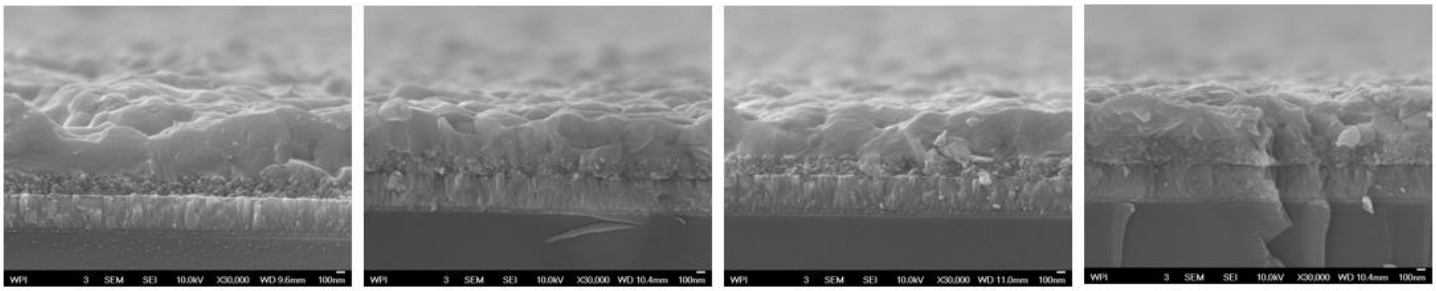

Figure 16: *SEM images of different samples that were compared. The glass-FTO interfaces do not line up.*

[1] This is unitless.

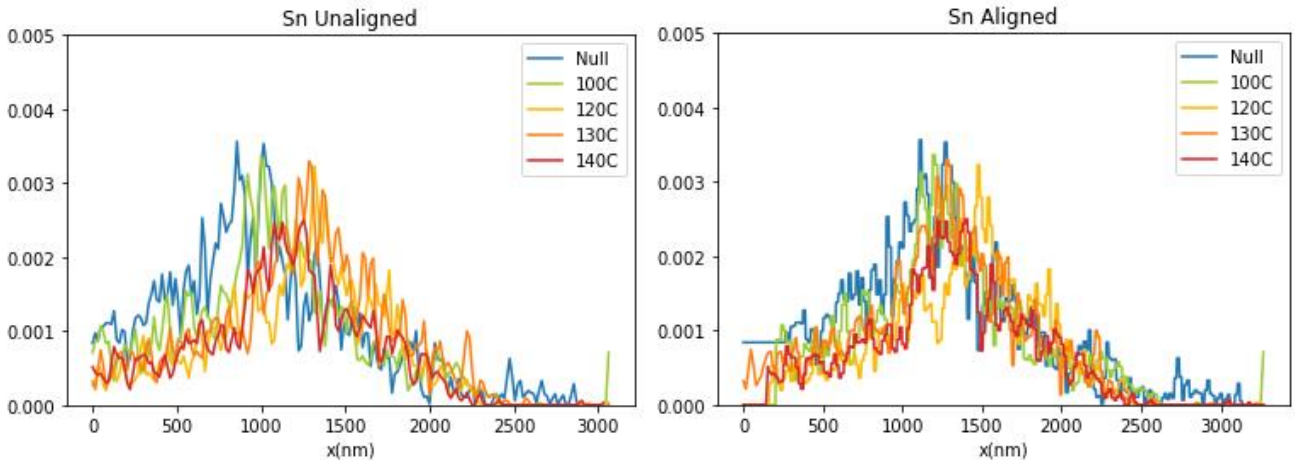

Figure 17: *Concentration profiles before (left) and after (right) the distances were aligned.*

Finally, the data were smoothed using a 50-point moving average - as shown in Figure 18[2] - to get rid of noise and make the graphs more readable. The python code and more detailed steps for this process can be found in Appendix 3.

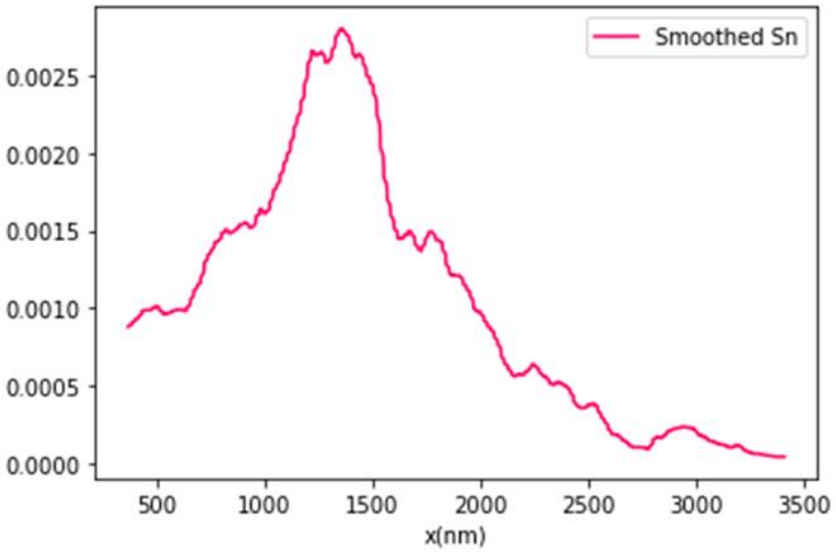

Figure 18: *The final, smoothed concentration profile of the image in Figure 14.*

[2] There are 773-780 data points per graph.

4.0 Results and Discussion

"More diffusion" refers to a larger spread in the concentration profile. The hypothesis for this project is that there will be more diffusion at higher temperatures, because there is more energy in the system, and more diffusion at longer timescales. Another thing to consider is that the diffusion may be asymmetric due to the different diffusivity constants of an element in different layers. Figure 19 shows some schematic concentration profiles to demonstrate these concepts.

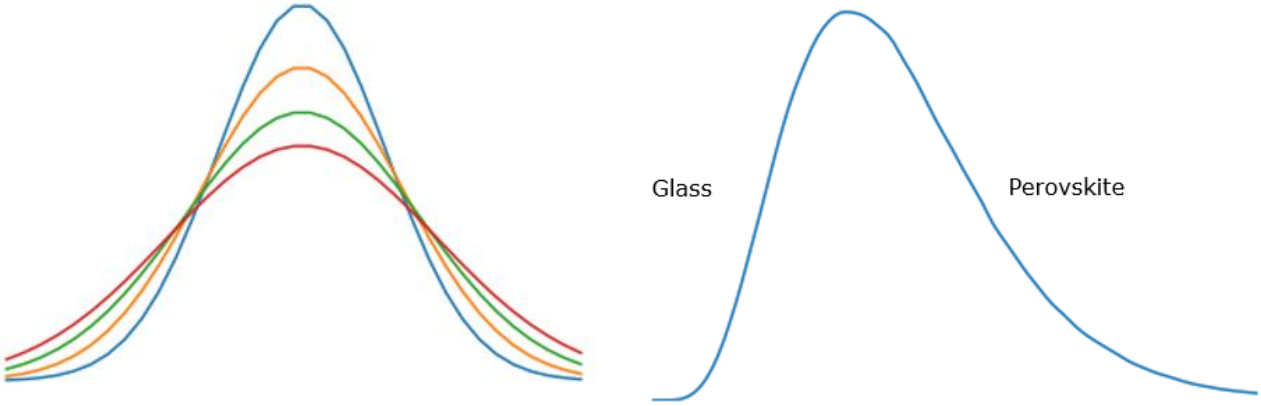

Figure 19: *On the left, concentration profiles with increasing spreads (blue to red), which indicate more diffusion at higher temperatures/longer times. On the right, an example of an asymmetric concentration profile, indicating different diffusivity constants of the element in different layers.*

The elements that are being examined are Sn, Ti, Pb, and I; Sn is expected to be found in the FTO layer, Ti in the ETL, and Pb and I in the perovskite layer. In Figures 20-22, these layer divisions are indicated by dashed purple lines; layer thickness between devices only varies by 50-80 nm and the divisions were determined by taking the average of these distances.

4.1 Different Annealing Times

Figure 20 shows the different concentration profiles for different annealing times at 130C. Sn shows the most intuitive results, with its peak shifting to the right for longer annealing times. The Ti peaks are also slightly shifted, but these results are still inconclusive. The I and Pb profiles show no clear trend in the position of the peaks, but large spreads to the unstable nature of the perovskite. The I has a larger spread than the Pb, due to the lower activation energy of vacancy migration (~0.1eV and ~0.8eV, respectively). Furthermore, all the elements have asymmetric concentration profiles which are consistent with different diffusivity constants in different layers.

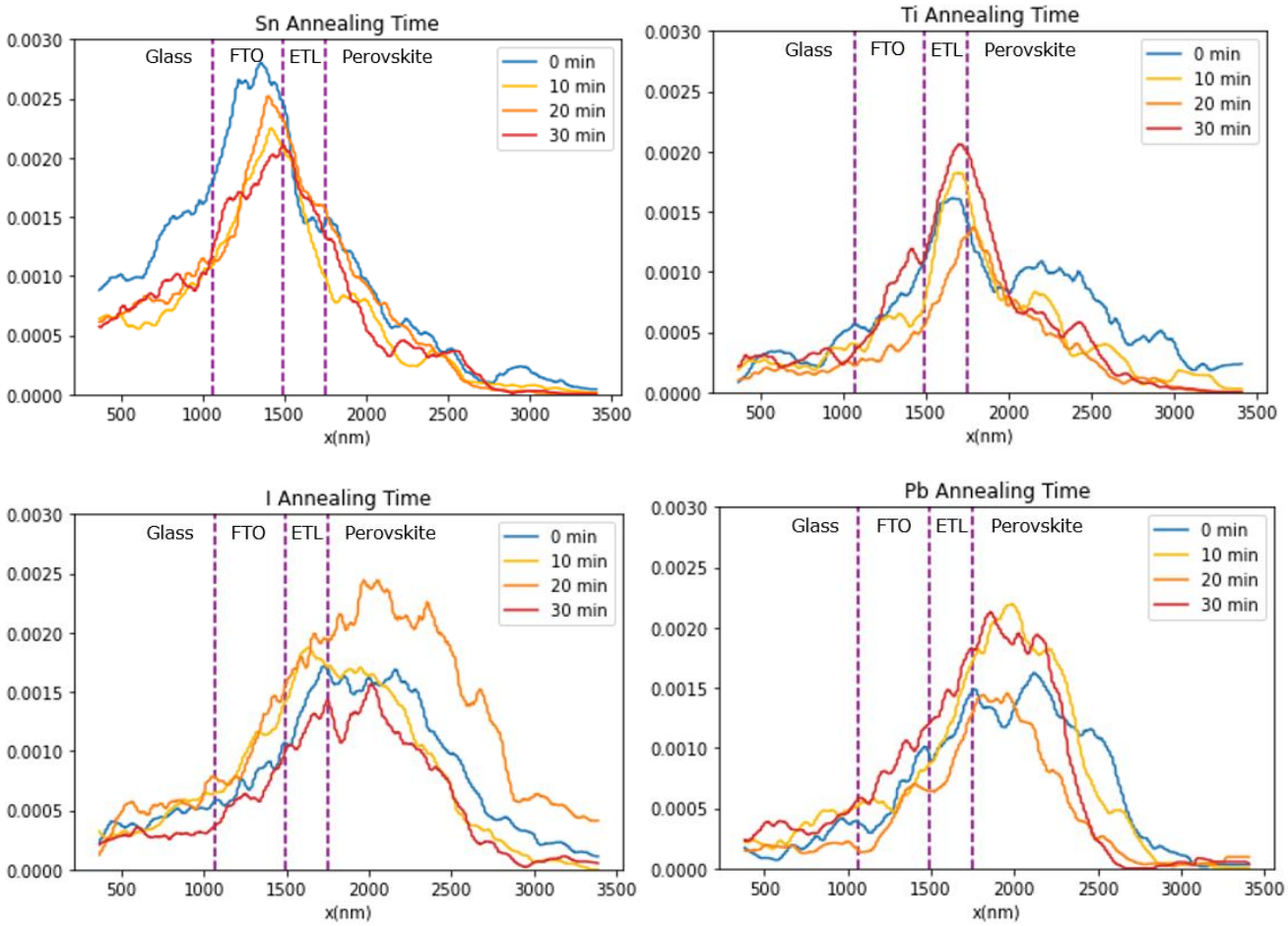

Figure 20: *The concentration profiles of each element for different annealing times at 130C. Sn shows a distinct shift in its peak as time increases, and I and Pb show very large spreads, consistent with the unstable nature of the perovskite layer.*

4.2 Different Annealing Temperatures

Figure 21 shows the results for different annealing temperatures. In each case, the sample was annealed for 20 min. These results are similar to those of the different annealing times, with the shifting peaks in Sn and broad spreads in I and Pb. One thing of note is the Ti profile, shown in Figure 22, where 100C is similar to no annealing ("Null"), but 120, 130, and 140C are shifted towards the perovskite layer.

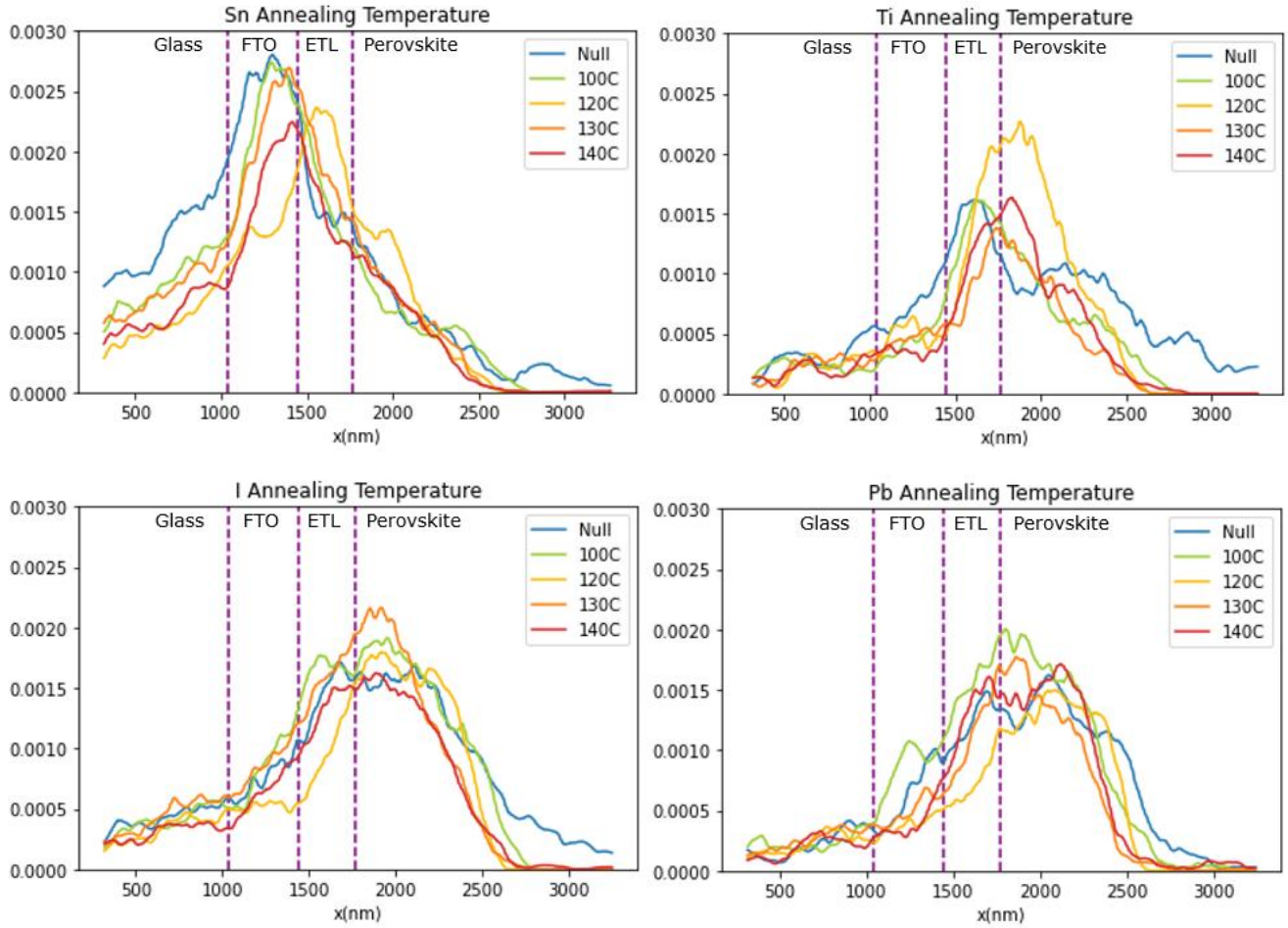

Figure 21: *The concentration profiles of the different elements for different annealing temperatures. The results are similar to those from Figure 20. The details of the Ti results are shown below in Figure 22.*

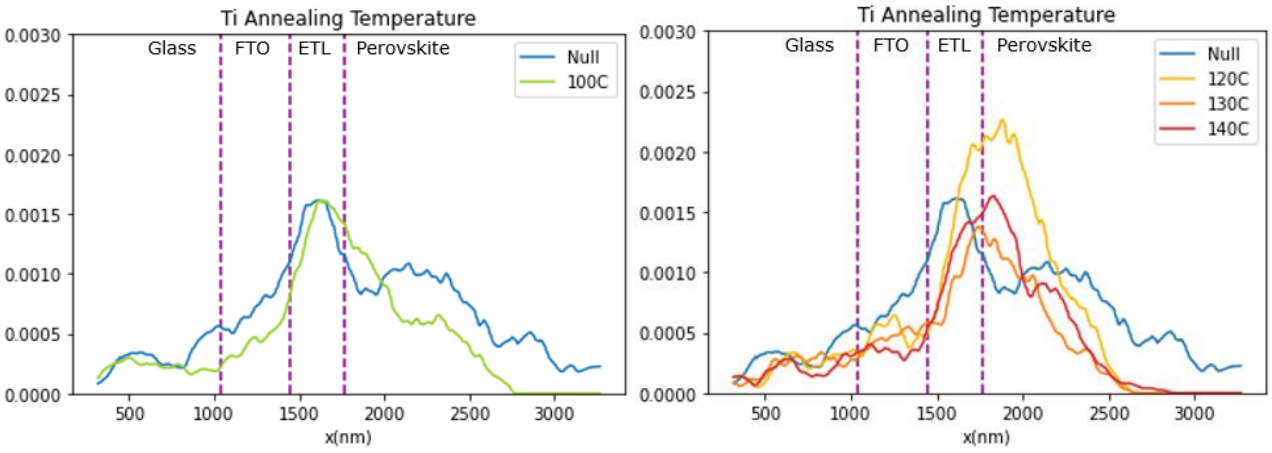

Figure 22: *On the left, Ti concentration profiles at 100C compared to no annealing ("Null"), where they have similar peaks. On the right, the higher temperatures compared to no annealing, where their peaks are shifted towards the perovskite.*

4.3 Sources of Error

In device fabrication, the amount of solution deposited before spin-coating varied from 65-80 uL, because the procedure only required that enough solution be used to cover the glass slide. Additionally, due to the availability of lab equipment, some layers on some devices were annealed on a hot plate that happened to be located inside a vacuum chamber. These two factors may have influenced the overall amount of an element in the device, indicated by the larger area under the concentration curve, but should not affect the diffusion trends.

For device characterization, there was some concern that the excitation volume of the EDS was detecting elements from other layers, as shown in Figure 23. The EDS maps are consistent with device structure, but this may affect how the concentration decays towards the top of the device. The devices may also not have been completely level when the maps were taken, adding a small uncertainty to the concentration profile. Furthermore, the images of the maps needed to be cropped such that there was no white space or text. To do so, some pixels at the edge of the maps may have been excluded, but this is negligible. Finally, all the results are only represented by one sample per condition, so further tests should be conducted to verify these results. Additional future work is presented in the next chapter.

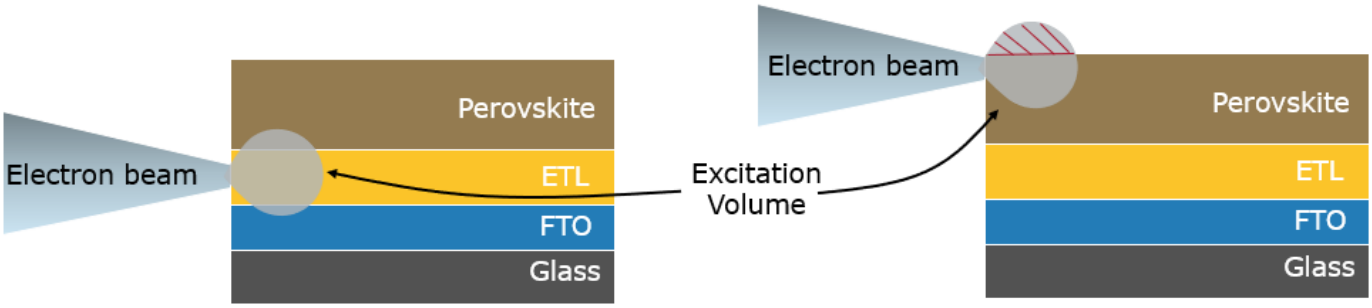

Figure 23: *A representation of the concern about the EDS excitation volume. On the left, the excitation volume is picking up information from different layers. On the right, the excitation volume falls outside of the device, which may affect how the concentration drops off on the right-hand side of Figures 20-22.*

5.0 Conclusion and Future Work

The goal of this project was to investigate the effects of annealing time and temperature of the perovskite layer in relation to the degradation of PSC devices. The existing method that was used to assess device composition only gave discrete snapshots of the weight percent of the elements within each layer, so a new analysis method was developed in order to obtain a continuous concentration profile; this gave more insight into device composition across the entire sample and at layer interfaces. When applied to samples that varied in annealing time and temperature, this method yielded results that are consistent with the literature; the shifts of Sn peaks with higher temperatures and longer times follow the diffusion theory of solids, and the large spreads of I and Pb are due to their low migration activation energies.

While the results of this project may not directly explain the mechanisms behind elemental diffusion-induced degradation of PSCs, it made an important first step in how to look at diffusion within a device. Most of the work done on this project was designing an experiment and an analysis method that produced results that could begin to show how diffusion influences long-term device stability, and the single run of data that were obtained are promising. However, given the short timeline of an MQP, especially in the time of the COVID-19 pandemic, the results should be validated in the near future.

5.1 Future Work

Further steps that could be done with these data include obtaining an average and uncertainty for concentration profiles with more than one sample, fitting the data to Fick's laws of diffusion, and extracting the diffusivity constants and migration activation energies of elements in different layers.

For future MQPs, some questions to consider are:

- How does the mass of a device change during annealing due to possible evaporation of the deposited solutions?
- What would the results of this experiment look like for a full device? Does adding the HTL create a large enough potential difference to facilitate ion migration?

- What do the concentration profiles look like after a device has been connected to an external circuit? How much of an effect does electrical current have on ion migration?
- For the above questions, how do these things affect how devices age? Do annealing conditions influence the concentration profiles after two days? A week? A month?
- The Energy Group has begun working with CsBr to aid in device stability. How does it affect the diffusion and kinetics occurring within the device?
- Is there a way to image/analyze diffusion occurring along grain boundaries?
- Does the SAM acting as an adhesion layer function as a diffusion barrier? If not, what could?

Overall, elemental diffusion is just one piece of the degradation puzzle that needs to be solved to improve the stability of PSCs for commercial use. Currently there are several solutions to improve device stability, but the root causes are not well understood. A possible solution is to combine all of the available methods known to improve device efficiency and stability: encapsulate devices in N_2 gas, use CsBr to improve stability of perovskite layer, use a graphene net to prevent I migration, and use the SAMs to improve contact and adhesion between the perovskite and ETL. Ideally, the analysis method developed herein can provide additional information about the elemental composition of devices to shed more light on how devices degrade, and how the aforementioned solutions improve device stability. If PSCs become commercially viable, they will have a profound impact on solar power efficiency and aid in the fight against climate change.

References

1. Kirchartz, T., Rau, U., What makes a good solar cell? *Adv. Energy Mater.* 2018, 8, 1703385. https://doi.org/10.1002/aenm.201703385
2. Hutter, E., Gélvez-Rueda, M., Osherov, A. *et al.* Direct–indirect character of the bandgap in methylammonium lead iodide perovskite. *Nature Mater* 16, 115–120 (2017). https://doi.org/10.1038/nmat4765
3. Wang, T., Daiber, B., Frost, J. et al. Indirect to direct bandgap transition in methylammonium lead halide perovskite. Energy Environ. Sci., 2017, 10, 509.
4. Bi, E., Chen, H., Xie, F. et al. 2017. Diffusion engineering of ions and charge carriers for stable efficient perovskite solar cells. *Nat Commun* 8, 15330 (2017). https://doi.org/10.1038/ncomms15330
5. Dong, W., Zhang, T., Chen, X., Wang, B., Zhu, B. 2017. Charge transport study of perovskite solar cells through constructing electron transport channels. Phys. Status Solidi A, 214: 1700089. https://doi.org/10.1002/pssa.201700089
6. Oyelade, O., Oyewole, O.K., Oyewole, D.O. *et al.* Pressure-Assisted Fabrication of Perovskite Solar Cells. *Sci Rep* 10, 7183 (2020). https://doi.org/10.1038/s41598-020-64090-5
7. Azpiroz, J., Mosconi, E., Bisquert, J., Angelis, F. 2015. Defect migration in methylammonium lead iodide and its role in perovskite solar cell operation. *Energy & Environmental Science* 8. https://doi.org/10.1039/C5EE01265A
8. Deretzis, I., Smecca, E., Mannino, G., et al. 2018. Stability and Degradation in Hybrid Perovskite: Is the Glass Half-Empty or Half-Full? *J. Phys. Chem. Lett.* 2018, 9, 11, 3000–3007. https://doi.org/10.1021/acs.jpclett.8b00120
9. Abbaschian, R., Abbaschian, L., Reed-Hill, R. (2009). *Physical Metallurgy Principles (4th ed.)*. Cengage Learning.
10. Figueres, C., Rivett-Carnac, T., Optimism, G., & The Future We Choose: Surviving the Climate Crisis. (2020, April 22). *How the World Will Look if We Don't Address Climate Change*. Time. https://time.com/5824295/climate-change-future-possibilities/.
11. *Undeniable signs of climate change: the human fingerprints*. Campaign against Climate Change. (2020, September 15). https://www.campaigncc.org/node/1201.

12. Gielen, D., Boshell, F., Saygin, D., Bazilian, M. D., Wagner, N., Ricardo Gorini. The role of renewable energy in the global energy transformation. *Energy Strategy Reviews*.Volume 24. 2019. https://doi.org/10.1016/j.esr.2019.01.006.
13. *The Paris Agreement*. unfccc.int. (n.d.). https://unfccc.int/process-and-meetings/the-paris-agreement/the-paris-agreement.
14. Gabbatiss, J. *Lobbying against key US climate regulation 'cost society $60bn,' study finds.* Carbon Brief. (2019, May 27). https://www.carbonbrief.org/lobbying-against-key-us-climate-regulation-cost-society-60bn-study-finds
15. Richardson, L.*What is the history of solar energy and when were solar panels invented?* EnergySage. (2018, May 3). https://news.energysage.com/the-history-and-invention-of-solar-panel-technology/
16. Carbeck, J. *Solar power has big limitations. This wonder material could change that.* World Economic Forum. (2016, June 23). https://www.weforum.org/agenda/2016/06/perovskite-solar-cells/
17. NREL. *Best Research-Cell Efficiencies*. (2021, March 30). https://www.nrel.gov/pv/assets/pdfs/best-research-cell-efficiencies.20200104.pdf
18. Askeland, D.R. (1996). Atom Movement in Materials. In: The Science and Engineering of Materials. Springer, Boston, MA. https://doi.org/10.1007/978-1-4899-2895-5_5
19. Wikipedia contributors. (2021, April 28). Mass diffusivity. In *Wikipedia, The Free Encyclopedia*. https://en.wikipedia.org/Mass_diffusivity
20. Wikipedia contributors. (2021, May 6). Diffusion. In *Wikipedia, The Free Encyclopedia*. https://en.wikipedia.org/wiki/Diffusion
21. Wikipedia contributors. (2021, May 1). Solar cell. In *Wikipedia, The Free Encyclopedia*. https://en.wikipedia.org/wiki/Solar_cell
22. Würfel, P. (2005). Basic Structure of Solar Cells. In Physics of Solar Cells, P. Würfel (Ed.). https://doi.org/10.1002/9783527618545.ch6
23. Nasir, B. (2021). Power Electronics.
24. Wikipedia contributors. 2021, May 4). P–n junction. In *Wikipedia, The Free Encyclopedia*. https://en.wikipedia.org/wiki/P%E2%80%93n_junction

25. Lopez-Varo, P., Jiménez-Tejada, J. A., García-Rosell, M., Ravishankar, S., Garcia-Belmonte, G., Bisquert, J., Almora, O., *Adv. Energy Mater.* 2018, 8, 1702772. https://doi.org/10.1002/aenm.201702772
26. Spies A., Reinhardt J., List M., Zimmermann B., Würfel U. (2017) Impact of Charge Carrier Mobility and Electrode Selectivity on the Performance of Organic Solar Cells. In: Leo K. (eds) Elementary Processes in Organic Photovoltaics. Advances in Polymer Science, vol 272. Springer, Cham. https://doi.org/10.1007/978-3-319-28338-8_17
27. Chen, P. *Absorption Coefficient*. (n.d) Solar Cells wiki page. https://sites.google.com/site/pengchenhomepage/wikipage/absorption_coef
28. Wikipedia contributors. (2021, April 18). Direct and indirect band gaps. In *Wikipedia, The Free Encyclopedia*. https://en.wikipedia.org/wiki/Direct_and_indirect_band_gaps
29. Bisquert, J., Juarez-Perez, E.J. The Causes of Degradation of Perovskite Solar Cells. *The Journal of Physical Chemistry Letters*. (2019) *10* (19), 5889-5891. DOI:10.1021/acs.jpclett.9b00613
30. Zu, F.-S., Amsalem, P., Salzmann, I., Wang, R.-B., Ralaiarisoa, M., Kowarik, S., Duhm, S., Koch, N., *Advanced Optical Materials* (2017), 5, 1700139.
31. Xu, R., Li, Y., Jin, T., Liu, Y., Bao, Q., O'Carroll, C., & Tang, J. In Situ Observation of Light Illumination-Induced Degradation in Organometal Mixed-Halide Perovskite Films. *ACS Applied Materials & Interfaces.* (2018). *10* (7), 6737-6746 DOI:10.1021/acsami.7b18389
32. Ralaiarisoa, M., Salzmann, I., Zu, F.-S., Koch, N., *Adv. Electron. Mater.* 2018, 4, 1800307. https://doi.org/10.1002/aelm.201800307
33. Mannino, G., Alberti, A., Deretzis, I., Smecca, E., Sanzaro, S., Numata, Y., Miyasaka, T., & La Magna, A. First Evidence of CH3NH3PbI3 Optical Constants Improvement in a N2 Environment in the Range 40–80 °C. *The Journal of Physical Chemistry*. C (2017) *121* (14), 7703-7710. DOI:10.1021/acs.jpcc.7b00764
34. Dai, Z., Yadavalli, S.K., Chen, M., Abbaspourtamijani, A., Qi, Y., Pasture, N.P. (2021). Interfacial toughening with self-assembled monolayers enhances perovskite solar cell reliability. *Science*. 372. DOI: 10.1126/science.abf5602

Appendix 1: Materials and Equipment

Table 1. Chemical properties of the compounds used for the c-TiO_2 of the experimental PSC.

Chemical Name	Chemical Formula	Molecular Weight (g/mol)	Density at 25C (g/mL)
Titanium diisopropoxide bis(acetylacetonate)	$[(CH_3)_2CHO]_2Ti(C_5H_7O_2)_2$	364.26	0.995
1-butanol	$C_4H_{10}O$	74.123	0.810

Table 2. Chemical properties of the compounds used for the perovskite layer of the experimental PSC.

Chemical Name	Chemical Formula	Molecular Weight (g/mol)	Mass Used (mg)	Volume Used (mL)
Lead Iodide	PbI_2	461.0	599.3	N/A
Formamidinium Iodide (FAI)	CH_5NI_2	172.0	60	N/A
Methylammonium Bromide	MABr	112.0	6.0	N/A
Methylammonium Chloride	CH_6ClN	67.02	6.0	N/A
Dimethylformamide (DMF)	$(CH_3)_2NCH$	73.09	N/A	0.95
Dimethyl Sulfide	C_2H_6S	62.13	N/A	0.05
Isopropyl Alcohol	C_3H_8O	60.1	N/A	1.00

Materials:

- FTO-coated glass
- CORNING PC-420D (hot plate)
- Laurell Technologies Corporation (spin coater)
- Easy-Vac-9 (dual stage vacuum pump)
- UN1066(compressed nitrogen)
- Detergent
- Acetone
- Isopropyl alcohol
- Ethanol

- JEOL JSM-7000F Field Emission Scanning Electron Microscope (SEM)
- NOVASCAN PSD Digital Pro Series Digital UV (Ozone system cleaner)
- Beakers
- Petri dishes (plastic)
- KEITHLEY 2400 SourceMeter

Appendix 2: Raw SEM and EDS Images

Different Annealing Times (at 130C)

0 min:

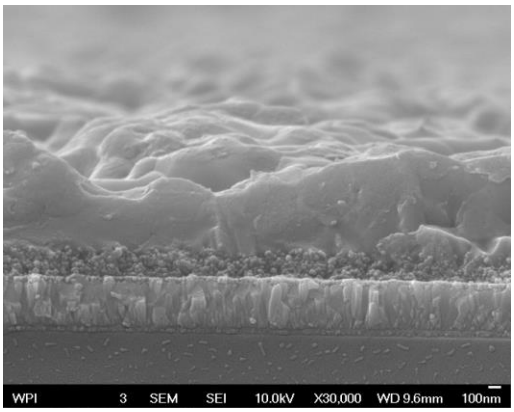

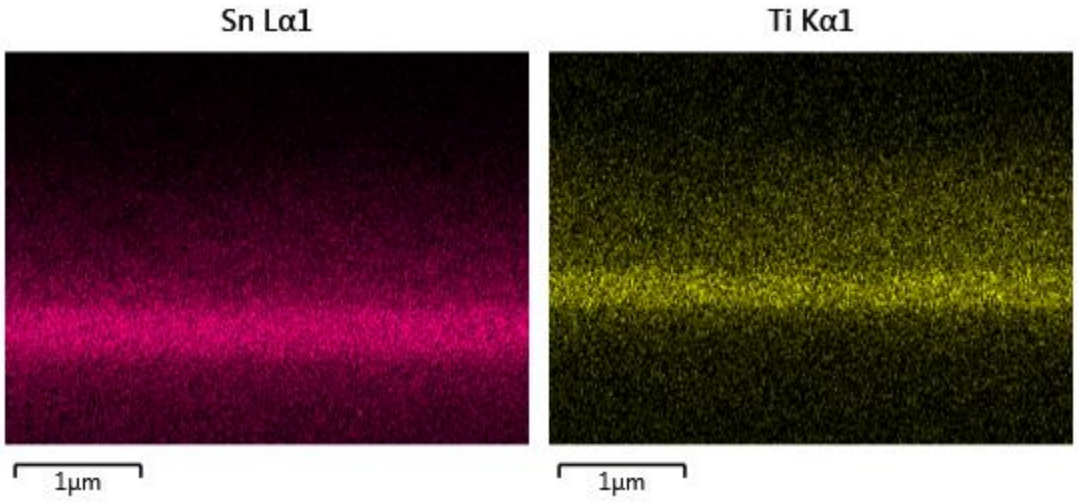

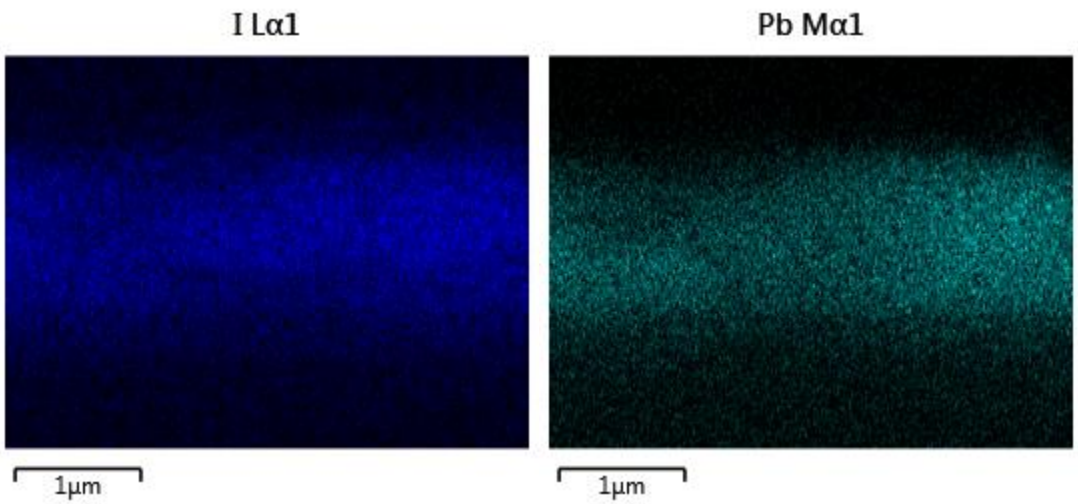

10 min:

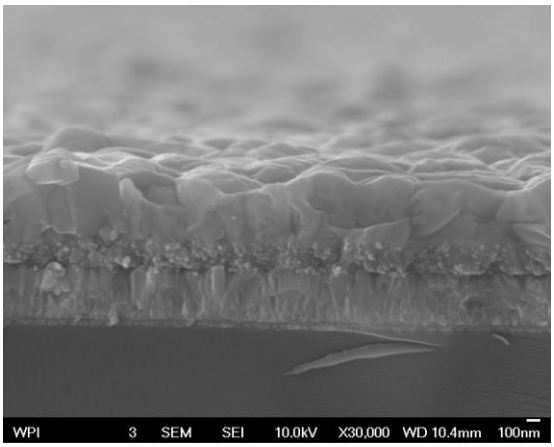
WPI 3 SEM SEI 10.0kV X30,000 WD 10.4mm 100nm

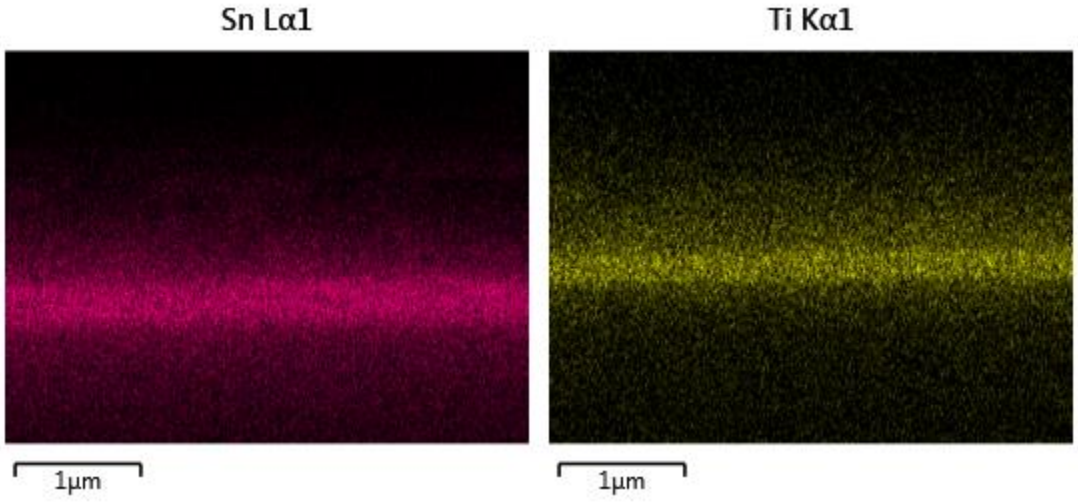
Sn Lα1
Ti Kα1
1µm
1µm

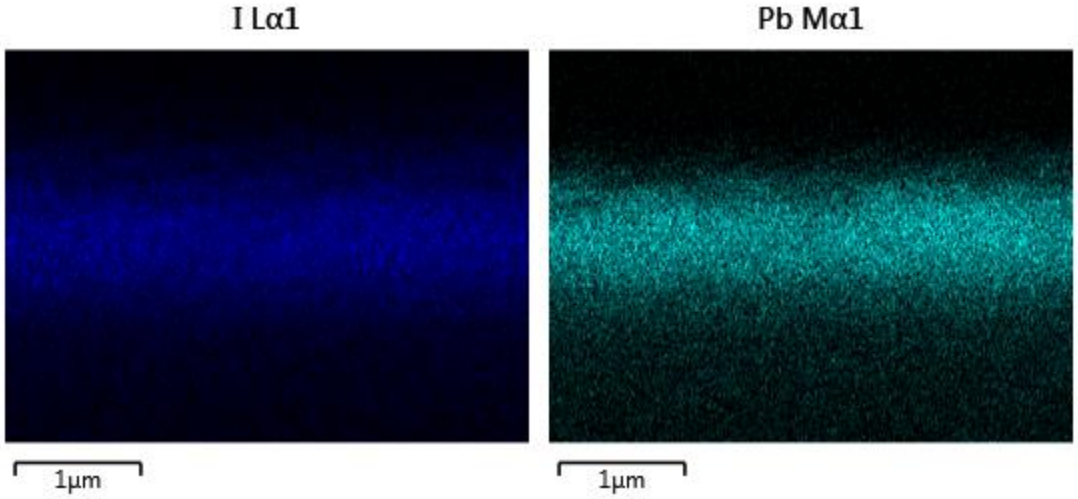
I Lα1
Pb Mα1
1µm
1µm

20 min:

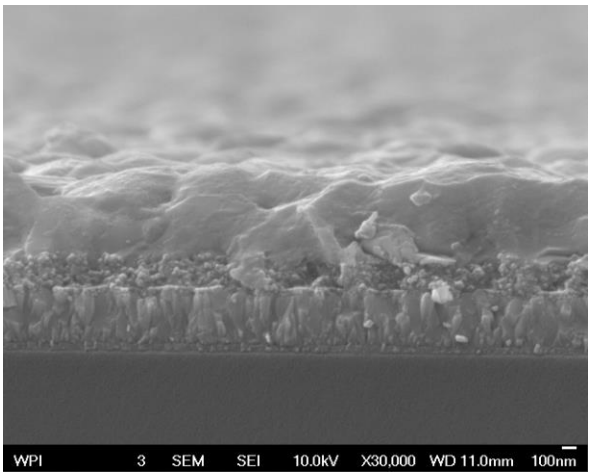
WPI 3 SEM SEI 10.0kV X30,000 WD 11.0mm 100nm

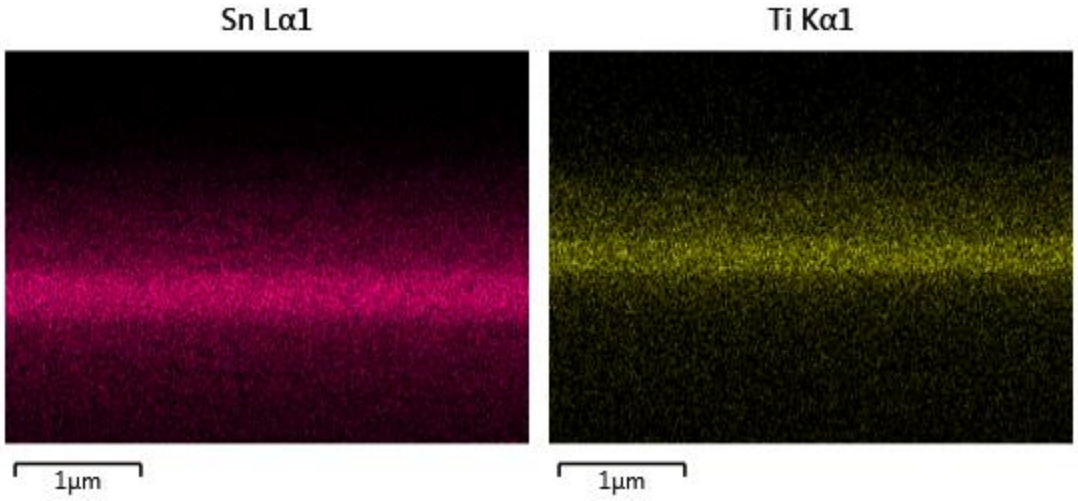
Sn Lα1
Ti Kα1
1µm
1µm

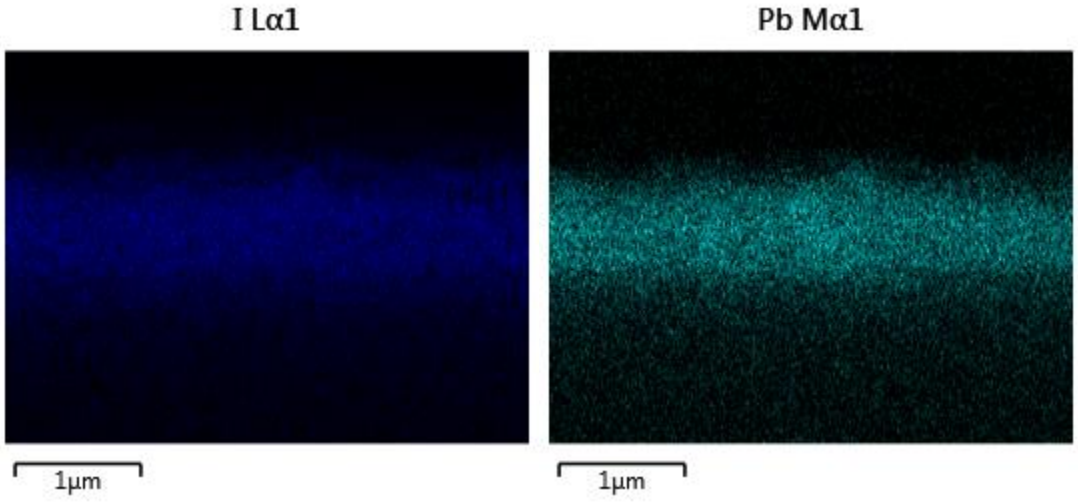
I Lα1
Pb Mα1
1µm
1µm

30 min:

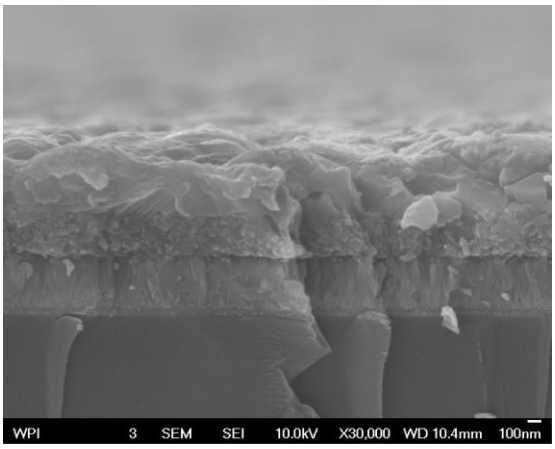
WPI 3 SEM SEI 10.0kV X30,000 WD 10.4mm 100nm

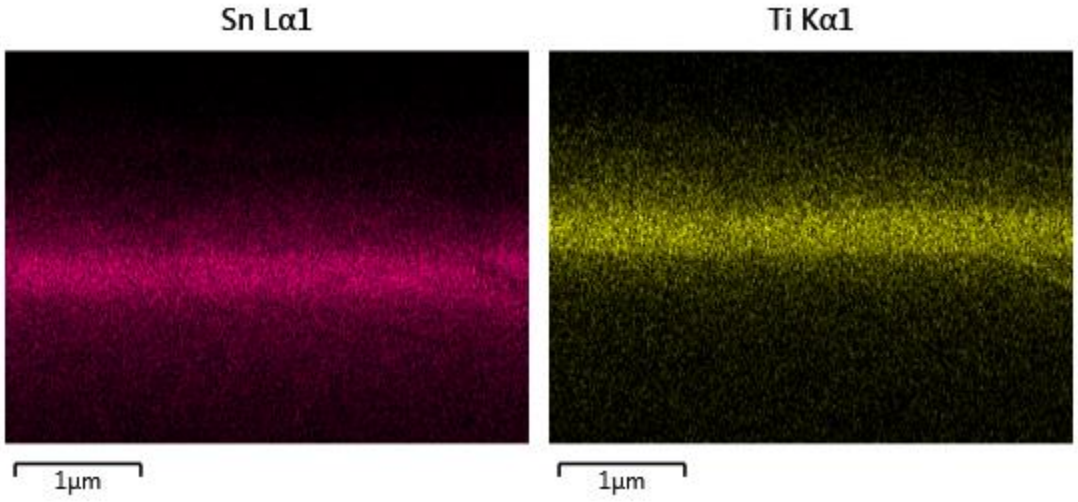
Sn Lα1
Ti Kα1
1µm
1µm

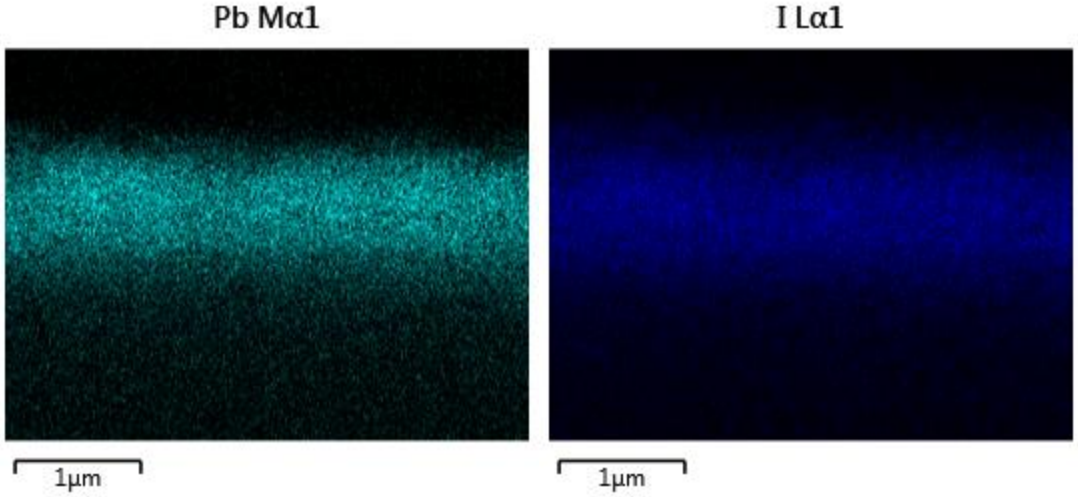
Pb Mα1
I Lα1
1µm
1µm

Different Annealing Temperatures (for 20 min)

100C:

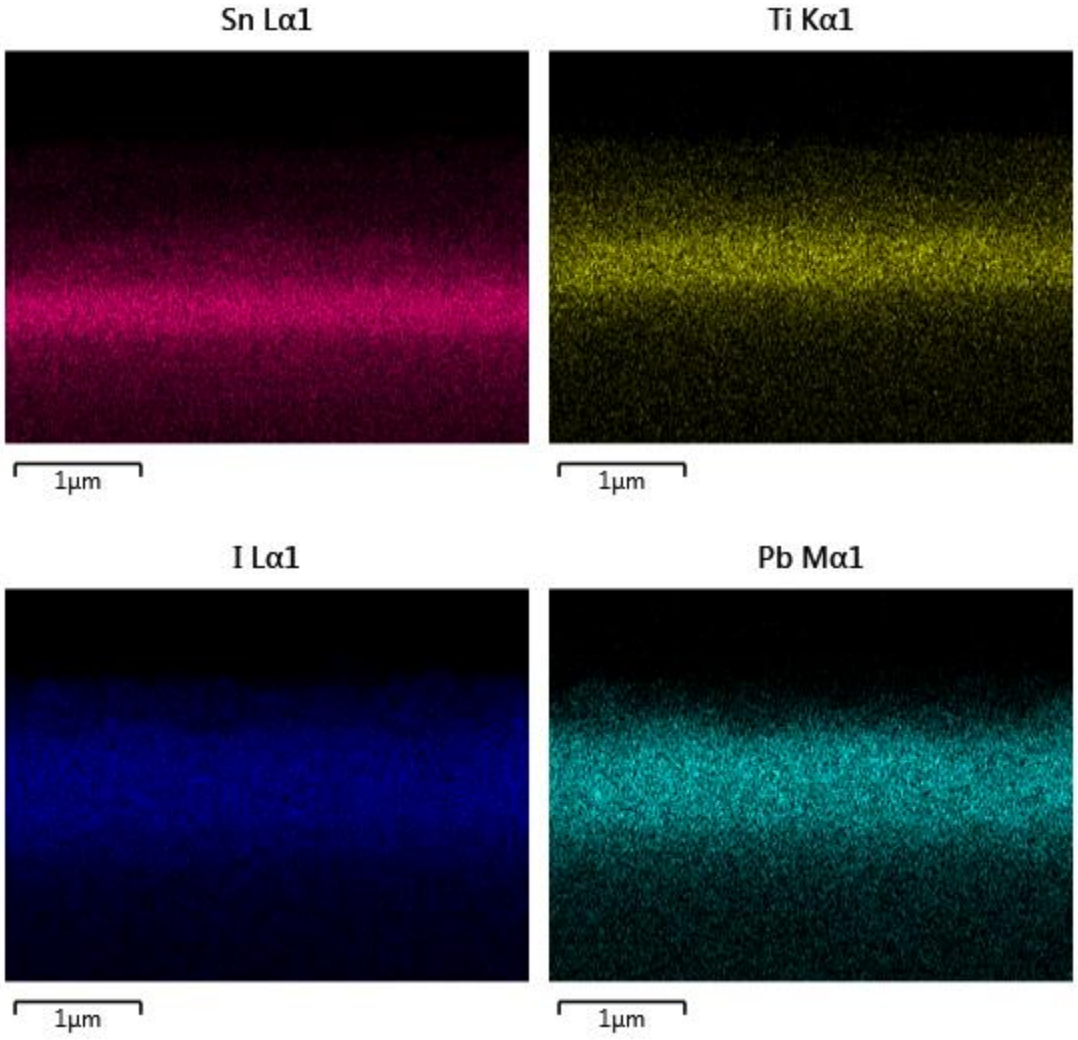

120C:

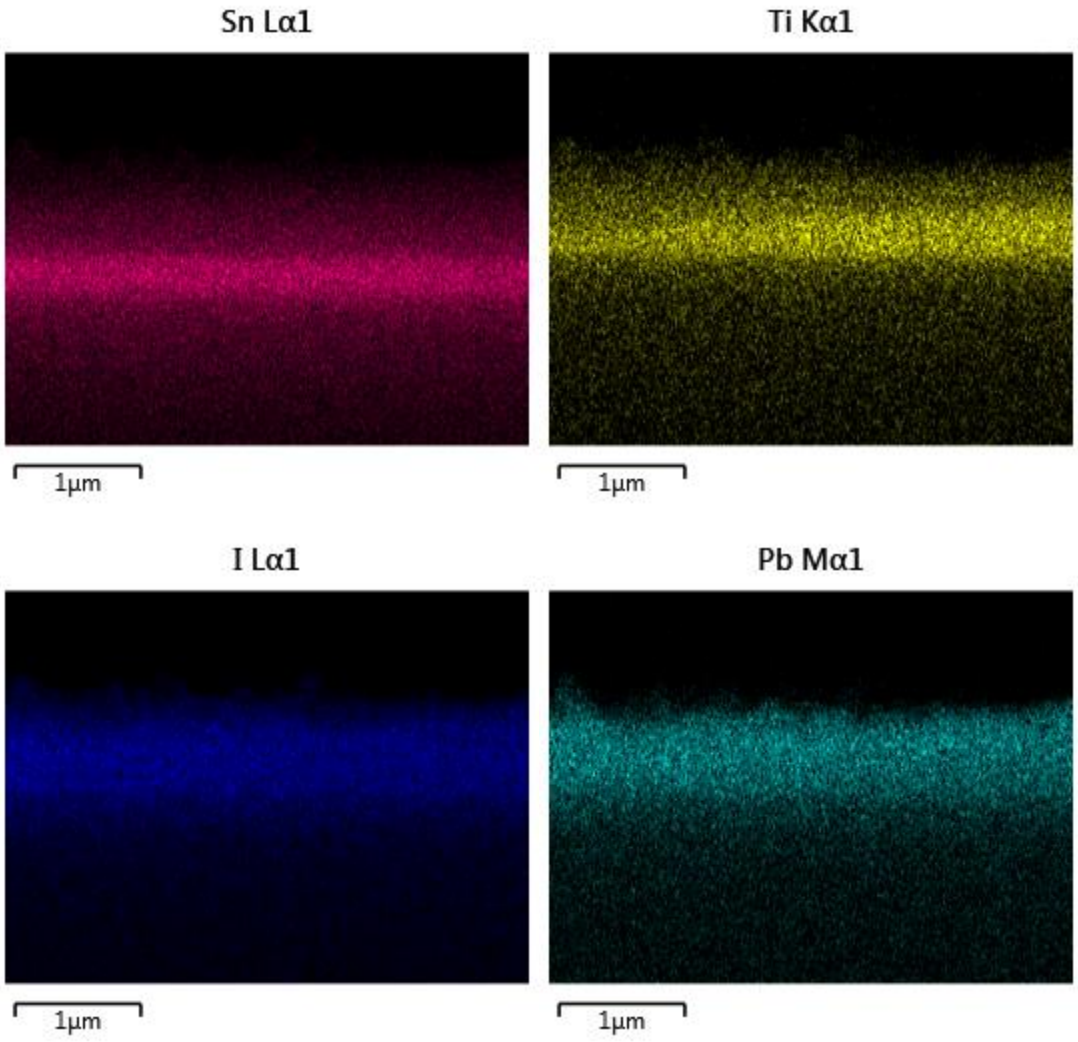

130C:

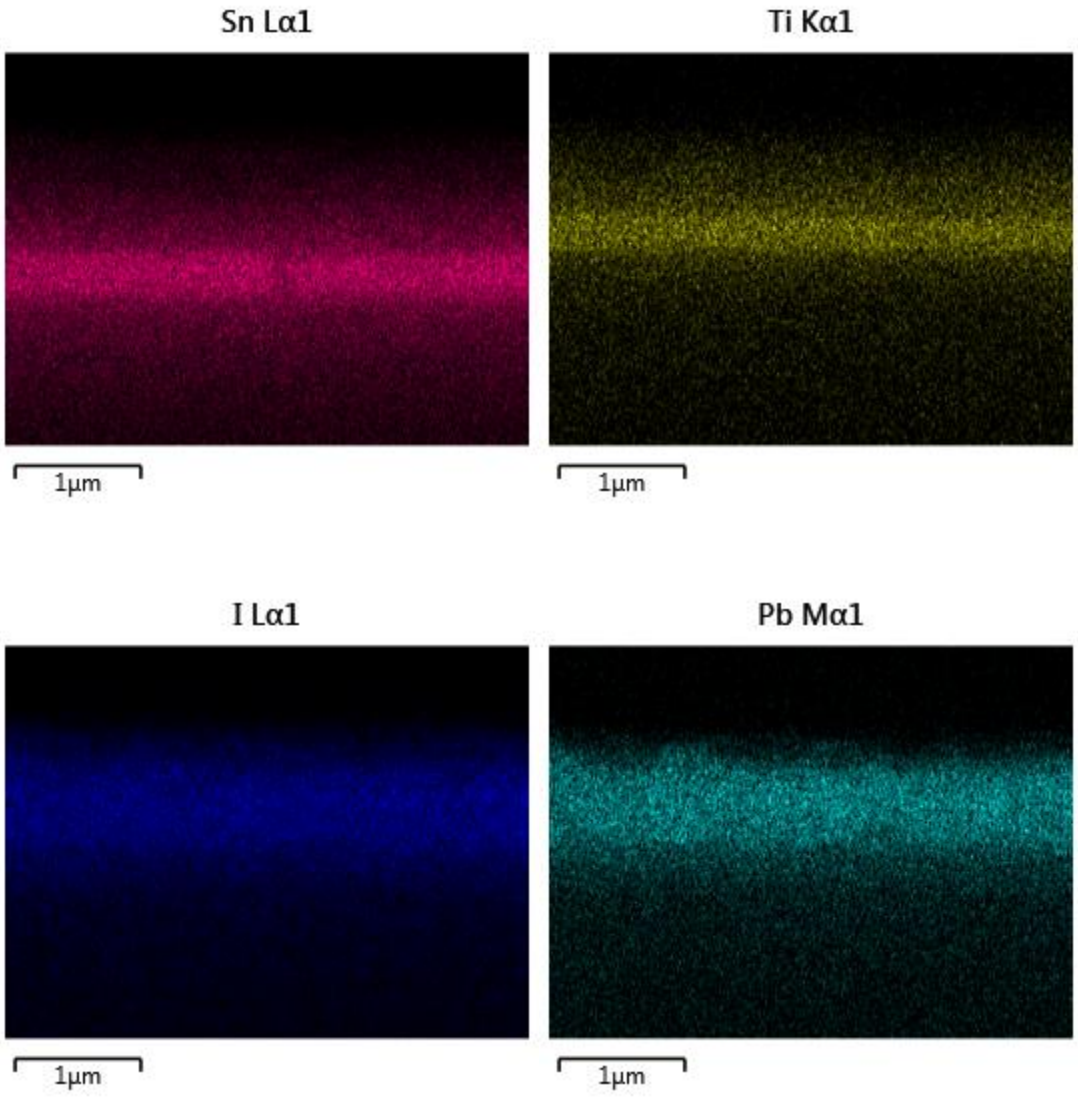

140C:

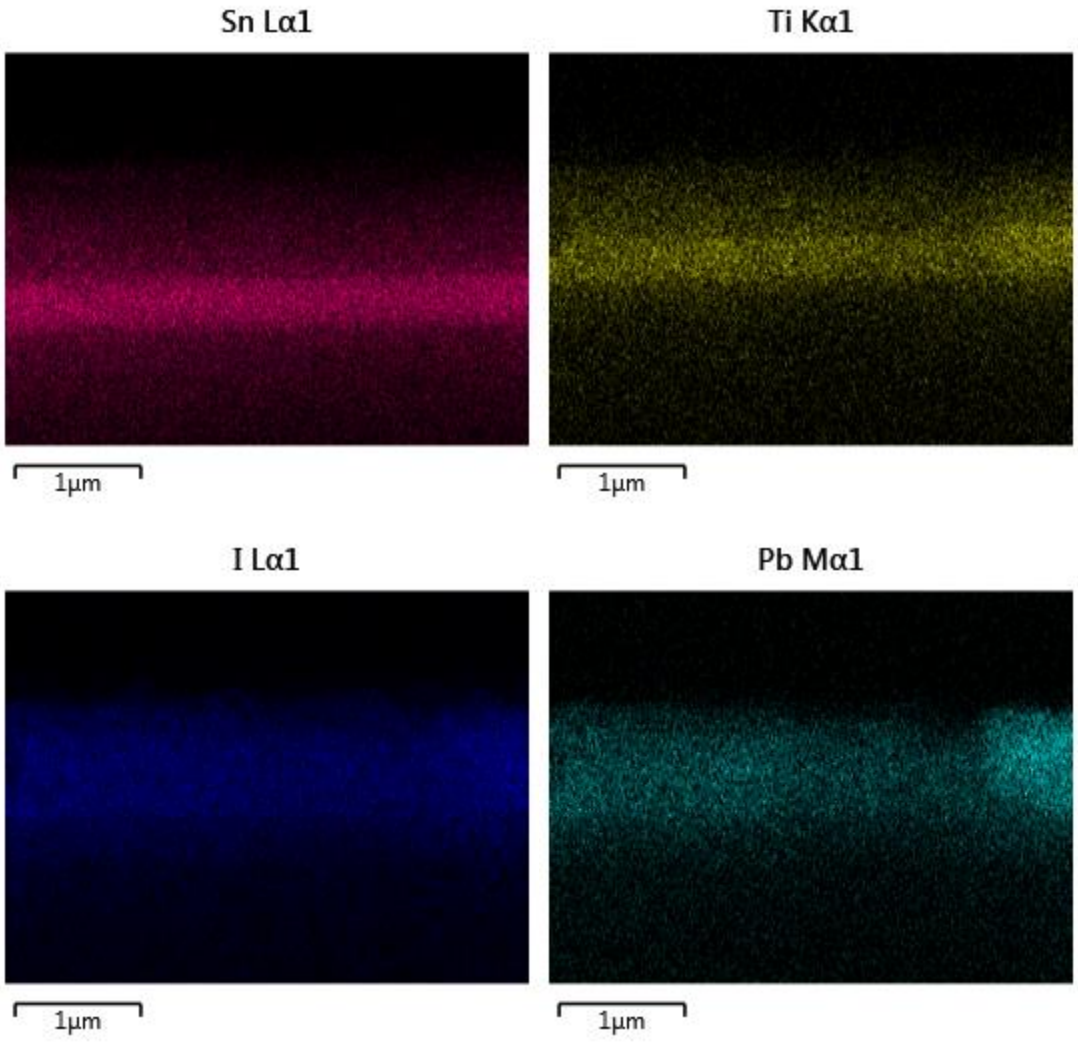

Appendix 3: Python Analysis

The code for this project was done in two different Python environments. Image processing was done in Processing.py (https://processing.org/download/), some data organization was done in Excel, and then graphed using Spyder (https://www.spyder-ide.org/). To obtain layer thicknesses, measurements were done on the SEM images using ImageJ (https://imagej.nih.gov/ij/download.html).

Python code in Processing.Py:

```
import csv

test = loadImage("I.png")

size(262, 196)

image(test, 0,0)


data = [['y', 'lum']]

for y in range(0,height):
    for x in range(0, width):
        Pixel = test.pixels[x + y*width]

        row = 0
        row += brightness(Pixel)/255


    data.append([y,row/width])

print(data)

f = open("test data.csv", 'w')

write = csv.writer(f)

write.writerows(data)

print("done")
```

This code wrote the data to a .csv file that was transferred to a master Excel sheet to align the distances and convert from pixels to nanometers.

Python code in Spyder:

```
# -*- coding: utf-8 -*-
"""
Spyder Editor

This is a temporary script file.
"""

import pandas as pd
import matplotlib.pyplot as plt
import tkinter as tk
from tkinter import filedialog

#read file
df = pd.DataFrame()
df_smooth = pd.DataFrame()
file_path = filedialog.askopenfilename()
xls = pd.ExcelFile(file_path)

sheets = xls.sheet_names

print(sheets)

loop = 'Y'
trial = input('Time or Temperature?: ')

while loop == 'Y':

    sheet = input('Enter Sheet Name: ')

    for x in sheets:
        if x == sheet:
            df = pd.read_excel(file_path, sheet_name=x)

    df_smooth['x(nm)'] = df['x(nm)']
    ind_var = 'x(nm)'
    columns = df.columns
```

```
    dep_vars = [] #0, 10, 20, 30 or 0, 100, 120, 130, 140
    #time colors
    colors = ['tab:blue', 'yellowgreen', '#fcba03', 'tab:orange', 'tab:red']
   #temp colors
    colors = []

    for col in columns:
        if col != ind_var:
            df_smooth[f'{col}'] = df[col].rolling(1).mean()
            dep_vars.append(f'{col}') #change for trial!!

    #w/ lines
    df_smooth.plot(x='x(nm)', y=dep_vars, color=colors)
    plt.title(sheet + trial) #' Annealing ' + trial)
    plt.ylim(0, .003)
    #glass/FTO
    plt.vlines(1037, 0, .003, colors='purple', linestyles='dashed')
    #FTO/ETL
    plt.vlines(1443, 0, .003, colors='purple', linestyles='dashed')
    #ETL/Perovskite
    plt.vlines(1766, 0, .003, colors='purple', linestyles='dashed')
    plt.ylim(0, .003)
    plt.show()
```

```
    #ind compared to 0
    for i in range(1, len(dep_vars)):
        df_smooth.plot(x='x(nm)', y=dep_vars[0], color=colors[0])
        plt.plot(df_smooth['x(nm)'], df_smooth[dep_vars[i]], label=dep_vars[i], color=colors[i])
        plt.title(sheet + ' Annealing ' + trial)
        plt.legend()
        #glass/FTO
        plt.vlines(1037, 0, .003, colors='purple', linestyles='dashed')
        #FTO/ETL
        plt.vlines(1443, 0, .003, colors='purple', linestyles='dashed')
        #ETL/Perovskite
        plt.vlines(1766, 0, .003, colors='purple', linestyles='dashed')
        plt.ylim(0, .003)
        plt.show()

    df_smooth.plot(x='x(nm)', y=dep_vars[0], color=colors[0])
    for i in range(2, len(dep_vars)):
        plt.plot(df_smooth['x(nm)'], df_smooth[dep_vars[i]], label=dep_vars[i], color=colors[i])

    plt.title(sheet + trial) # + ' Annealing ' + trial)
    plt.legend()
    #glass/FTO
    plt.vlines(1037, 0, .003, colors='purple', linestyles='dashed')
    #FTO/ETL
    plt.vlines(1443, 0, .003, colors='purple', linestyles='dashed')
    #ETL/Perovskite
    plt.vlines(1766, 0, .003, colors='purple', linestyles='dashed')
    plt.ylim(0, .003)
    plt.show()

    loop = input('Continue? (Y/N): ')
```